ISSN 0869-5911, Petrology, 2018, Vol. 26, No. 6, pp. 617–639. © Pleiades Publishing, Ltd., 2018.
Original Russian Text © O.G. Safonov, D.D. van Reenen, V.O. Yapaskurt, D.A. Varlamov, A.S. Mityaev, V.G. Butvina, M.A. Golunova, G.A. Belyanin, C.A. Smit, 2018, published in Petrologiya, 2018, Vol. 26, No. 6, pp. 633–658.

Thermal and Fluid Effects of Granitoid Intrusions on Granulite Complexes: Examples from the Southern Marginal Zone of the Limpopo Complex, South Africa

O. G. Safonov[a, b, c, *], **D. D. van Reenen**[c], **V. O. Yapaskurt**[a, b], **D. A. Varlamov**[a], **A. S. Mityaev**[a, b], **V. G. Butvina**[a], **M. A. Golunova**[a], **G. A. Belyanin**[c], **and C. A. Smit**[c]

[a]*Korzhinskii Institute of Experimental Mineralogy (IEM), Russian Academy of Sciences, Chernogolovka, Moscow oblast, 142432 Russia*

[b]*Geological Faculty, Moscow State University, Moscow, 119899 Russia*

[c]*Department of Geology, University of Johannesburg PO Box 524, Auckland Park, 2006, Johannesburg, South Africa*

**e-mail: oleg@iem.ac.ru*

Received May 12, 2018; in final form, June 21, 2018

Abstract—The paper summarizes data on the petrology of granitoid intrusions in the Southern Marginal Zone (SMZ) of the Neoarchean Limpopo granulite complex, South Africa, and discusses the thermal and fluid effects of these intrusions on the granulites. The intrusions were emplaced in SMZ at 2680–2640 Ma, when the granulite complex was overthrust on the rocks of the adjacent Kaapvaal Craton. The mineral assemblages of the granitoids reflect temperatures above 900°C for the magmas that crystallized under pressures of 6–9 kbar. The granitoid magmas assimilated host rocks and were thereby enriched in MgO, FeO, and Al_2O_3, which was favorable for the crystallization of garnet, spinel, sillimanite, and corundum in the granitoids. Fluid inclusions in the granitoids and estimates of the fluid composition based on mineral equilibria indicate that the CO_2/H_2O ratio of the fluids broadly varied. Along with H_2O–CO_2 fluid, the magmas carried H_2O–salt fluids, which penetrated the host rocks and triggered various metasomatic reactions in them. The thermal effects of the intrusions on the host granulites resulted in the development of partial melting zones that host orthopyroxene with >7 wt % Al_2O_3. Depending on the fluid regime and temperature, the orthopyroxene is found in equilibrium with either garnet and potassic feldspar or with biotite. The ages of the partial melting zones are comparable with those of the intrusions.

Keywords: granulite complexes, granitoids, H_2O–CO_2 fluids, H_2O–salt fluids, anatexis, fluid–mineral reactions, *P–T* parameters of metamorphism

DOI: 10.1134/S0869591118060061

INTRODUCTION

Granitoid magmatism was associated with the redistribution of material between various crustal levels, and this stabilized the structure of the crust (Sawyer et al., 2011; Brown, 2013). Archean and Proterozoic crustal domains metamorphosed to the granulite facies are usually characterized by active and compositionally diverse granitoid magmatism, which occurs as multiple and relatively brief pulses (see reviews in Kemp and Hawkesworth, 2003; Condie et al., 2009; Halla et al., 2017). Because of this, granite magmas are often thought to be derived in relation to granulite metamorphism in the lower and middle crust. Granulites are thereby formed as residues depleted in volatile and lithophile elements of the partial melting of compositionally diverse crustal rocks during prograde metamorphism (Clemens, 1990; Vielzeuf et al., 1990; Brown, 2006; Sawyer et al., 2011; Taylor et al., 2014). However, extensive field, geochronologic, and geochemical data indicate that significant volumes of granite magmas are emplaced in Precambrian granite complexes not only during their prograde metamorphism but also at metamorphic peaks and even during retrogression (Jung et al., 1998; Barbosa et al., 2006; Perchuk et al., 2008b; Huizenga et al., 2011; Laurent et al., 2014; Morfin et al., 2013, 2014; van Reenen et al., 2014; Safonov et al., 2014). The sources of the magmas might have been unrelated to the host granulites. These complexes were suggested to be referred to as *injection complexes* (Weinberg and Searle, 1998; Morfin et al., 2013, 2014). A defining feature of injection compositions is that they were emplaced into ductile rocks, whose temperatures were comparable to the temperatures of the intrusions.

However, the effect of granitoid intrusions is often underestimated in current models for the evolution of certain granulite complexes. These effects can be summarized as follows. First, these granitoid magmas, which were brought from anatexis regions at deeper and often also hotter crustal levels, were able to produce zones of (ultra)high-temperature metamorphism and/or partial melting in granulite complexes. Second, the hot magmas could assimilate host granulites and thus modify both their major, trace element and isotopic compositions and these characteristics of the host rocks. Third, granitoid magmas commonly carried vast volumes of fluids, which were released when the magmas crystallized and changed the geochemistry of the host rocks and produced new mineral assemblages in these rocks.

This publication summarizes our earlier data (Safonov et al., 2014, 2018a, 2018b) acquired by studying granulites in the Southern Marginal Zone (SMZ) of the Limpopo granulite complex in South Africa. These data demonstrate the thermal and fluid effects of synmetamorphic granitoid intrusions ascending from the lower crust.

GEOLOGY AND METAMORPHIC EVOLUTION OF THE SOUTHERN MARGINAL ZONE OF THE LIMPOPO COMPLEX

The Limpopo granulite complex in South Africa is a classic example of Neoarchean fold area formed between two cratons: Zimbabwe in the north and Kaapvaal in the south (Fig. 1). Based on structural and lithological features of rocks composing the Limpopo Complex, it is subdivided into the Northern Marginal Zone (NMZ), Central Zone (CZ), and Southern Marginal Zone (SMZ), which are separated by large regional-scale shear zones (Fig. 1). The Central Zone shows evidence of multiple metamorphic events (Perchuk et al., 2008a; Smit et al., 2011; Kramers et al., 2011; Brandt et al., 2018; Kröner et al., 2018), whereas the Northern and Southern Marginal Zones were affected only by one stage of granulite metamorphism and are regarded by many researchers as high-grade equivalents of granite–greenstone complexes of adjacent cratons (Kreissig et al., 2000, 2001; Blenkinsop, 2011; van Reenen et al., 2011, 2014). The Northern Zone is dominated by large intrusive charnockite–enderbite complexes and supracrustal rock sequences, which were dated within the range of 2740–2570 Ma (Blenkinsop, 2011).

The Southern Marginal Zone, to which this publication is devoted, is adjacent to the northern block (Pietersburg block) of the Kaapvaal Craton in the south along the gently dipping Hout River regional shear zone (Fig. 1). This long zone started to develop between 2720 and 2690 Ma and controlled the thrusting of the SMZ granulites over granite–greenstone belts of the craton (Kreissig et al., 2001; van Reenen et al., 2011; Kramers et al., 2014; Smit et al., 2014). The SMZ rocks metamorphosed to the granulite facies make up the hanging wall of the Hout River Shear Zone, whereas the low-grade (metamorphosed to the greenschist and amphibolite facies) rocks of the Kaapvaal Craton compose its footwall. The SMZ is composed of two major lithological associations (see, for example, van Reenen et al., 2011, 2014): (1) strongly deformed migmatized Bavianskloof tonalite–trondhjemite gneisses and (2) the Bandelierkop Formation, which comprises ultramafic and mafic granulites, metapelites, and BIF. These formations compose large blocks bounded by regional shear zones (Annaskraal, Petronella, and Matok) (Fig. 1) (Smit et al., 2014; Smit and van Reenen, 1997). Based on the bulk compositions of the rocks, their trace-element geochemistry, and their Nd and Pb, isotopic compositions, Kreissig et al. (2000, 2001) arrived at the conclusion that the SMZ granulites are geochemical analogues of supracrustal rocks of greenstone belts of the Pietersburg block of the Kaapvaal Craton. This conclusion is corroborated by the age of detrital zircons (3440 Ma) from the Bandelierkop metapelite formation, which is within the age range of ancient sedimentary complexes of the Kaapvaal Craton (see, for example, Zeh et al., 2013). However, the metapelites of the Bandelierkop Formation also contain zircons, which were dated at below 3000 Ma (Rajesh et al., 2014; Nicoli et al., 2015) and thus provide grounds to conclude that the metasediments of this formation were not anyhow related to the craton but make up a separate block, which was amalgamated to the Kaapvaal Craton by collision (Nicoli et al., 2015).

The metamorphic peak in SMZ, in both the Bavianskloof gneisses and the Bandelierkop Formation, occurred at 2710–2720 Ma (Retief et al., 1990; Belyanin et al., 2014; Rajesh et al., 2014; Taylor et al., 2014; Nicoli et al., 2015), thus highlighting their common metamorphic history. Conventional mineral thermobarometry and the modeling of mineral assemblages using pseudosections suggest temperatures of 800–870°C and pressures of 7.5–11 kbar for the metamorphic peak in SMZ (see, for example, van Reenen, 1983; Stevens, van Reenen, 1992; Perchuk et al., 1996, 2000; Taylor et al., 2014; Nicoli et al., 2015). Some researchers (for example, Stevens, van Reenen, 1992; Taylor et al., 2014; Nicoli et al., 2015) are prone to think that the metamorphic peak in SMZ was reached along an anticlockwise P–T path, which corresponded to the burial of the rocks to the basement of the continental crust and their heating at collision. Some geologists (Tsunogae et al., 2004, Belyanin et al., 2012; Rajesh et al., 2014) pointed out that ultrahigh-temperature (>1000°C at 11–12 kbar) metamorphic parameters were reached at the metamorphic peak in SMZ, while other authors (for example, Taylor et al., 2014; Nicoli et al., 2015) sharply criticized this conclusion.

The metamorphic evolution of SMZ after the peak of metamorphism, at 2720–2690 Ma, was controlled by the exhumation of the granulites and by the thrusting of the hot granulite allochthon over the Kaapvaal Craton along the Hout River Shear Zone (Smit et al., 2001, 2014; van Reenen et al., 2011, 2014). The

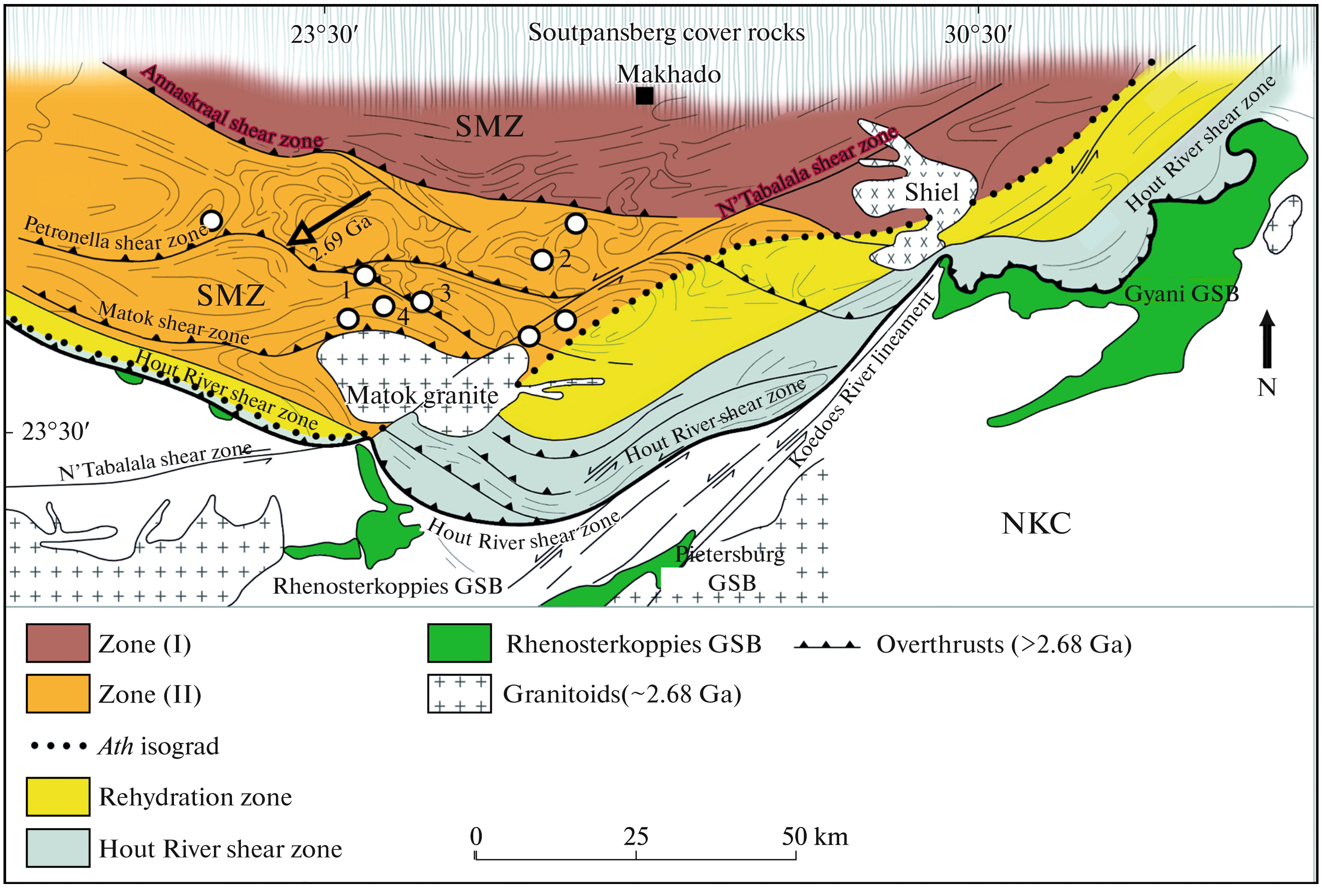

Fig. 1. Schematic geological map of the Southern Marginal Zone (SMZ) of the Limpopo Complex. The map displays major tectono-lithological features, metamorphic zones, and intrusive complexes. Open circles mark the largest intrusive massifs of garnet-bearing leucocratic granites, including the following massifs mentioned in the text: (1) Petronella, (2) Bandelierkop, (3) Klipputs, and (4) Koppieskraal. Zone (I) is the metamorphic zone in which petrological evidence was recovered of decompressional cooling *P–T* trajectories, Zone (II) is the metaamorphic zone in which petrological evidence was recovered of *P–T* trajectories of both decompressional cooling and subsequent subisobaric cooling. The arrow labeled 2.69 Ga indicates the thrusting direction of SMZ on the Kaapvaal Craton. SZ are shear zones, GSB is greenstone belts, and NKC is the northern marginal block of the Kaapvaal Craton.

decompression episode was dated at 2691 ± 7 Ma by U-Pb method on monazite, which occurs in association with corona reaction textures typical of this process. The coronas in the metapelites were produced by the reaction *Grt* + *Qz* = *Opx* + *Crd* (Kreissig et al., 2001). While rocks of the complex north of the Annaskraal shear zone (zone I in Fig. 1) show petrological evidence mostly of decompression-cooling *P–T* trajectories (see, for example, van Reenen et al., 2011, 2014), metapelites of the Bandelierkop Formation south of this zone (Zone II) preserve evidence of subsequent isobaric cooling at pressures of 6.0–6.5 kbar: these are reaction textures with garnet replacing cordierite according to the reaction *Crd* = *Grt* + *Sil* + *Qz* (van Reenen, 1983; Stevens and van Reenen, 1992; Perchuk et al., 1996, 2000; Smit et al., 2001, 2014; Taylor et al., 2014; Nicoli et al., 2015; van Reenen et al., 2011, 2014; Safonov et al., 2014). Subisobaric cooling reflects the nearly horizontal thrusting of the granulites over the craton, a process that continued until approximately 2620 Ma. Subisobaric cooling was associated with regional dehydration of the granulites in the hanging wall of the Hout River Shear Zone and the establishment of the "orthoamphibole isograd" (van Reenen, 1986; Stevens, 1997; van Reenen et al., 2011; 2014; Smit et al., 2014; Koizumi et al., 2014), which is defined by the widespread association *Opx* + *Ath* + *Qz* in the metapelites (Fig. 1). The Ar–Ar amphibole (from the mafic granulite) age of the rehydration process is 2660–2670 Ma (Belyanin et al., 2014). This process was controlled by the influx of fluids into the granulites. The fluids contained both CO_2 and H_2O–salt constituents (van Reenen, 1986; van Reenen and Hollister, 1988; Baker et al., 1992; van den Berg and Huizenga, 2001; Huizenga et al., 2014; van Reenen et al., 2014) and were likely derived from rocks of greenstone belts of the Kaapvaal Craton that were thrust beneath the SMZ granulites (van Reenen, 1986; van Reenen and Hollister, 1988; Smit et al., 2014; van

Table 1. Representative compositions (wt %) of the garnet-bearing leucocratic granitoids in the Southern Marginal Zone of the Limpopo Complex

Oxide	Bandelierkop						Petronella			Koppieskraal		Klipputs	
	SA-4-6A[(1)]	L14-7-1[(2)]	L14-7-5[(2)]	L3a[(3)]	L3d[(3)]	BD-C5[(3)]	PET6[(4)]	PET10[(4)]	PET11[(4)]	17-16	17-19	17-24	17-25
SiO_2	69.24	68.95	71.79	73.5	77.3	71.9	69.75	75.40	75.65	69.39	72.73	71.46	73.84
TiO_2	0.07	0.03	0.47	0.10	0.10	0.10	–	–	–	0.01	0.02	0.03	0.02
Al_2O_3	17.78	16.11	14.78	15.9	14.1	15.6	17.60	13.31	14.01	17.35	15.18	16.21	14.87
Fe_2O_3	0.80	3.16	3.94	0.90	0.60	0.20	0.35	1.90	0.60	0.63	0.67	1.37	1.16
MnO	0.01	0.00	0.00	0.00	0.00	0.00	–	0.54	0.19	0.02	0.01	0.03	0.02
MgO	0.18	1.06	1.33	0.20	0.20	0.10	–	–	–	0.10	0.05	0.21	0.28
CaO	1.86	0.69	2.11	1.30	1.40	1.50	2.33	1.89	2.10	0.71	0.53	1.57	1.06
Na_2O	5.47	3.22	4.19	3.70	4.00	4.00	6.49	4.45	4.92	6.34	4.97	5.16	5.06
K_2O	3.10	5.36	1.01	2.00	1.80	3.60	1.59	0.72	0.80	4.41	5.17	3.18	2.86
P_2O_5	0.12	0.09	0.15	0.1	0.1	0.1	0.08	–	–	0.06	0.03	0.07	0.07

Samples: [(1)] Dubinina et al. (2015), [(2)] Safonov et al. (2018b), [(3)] Taylor et al. (2014), [(4)] Safonov et al. (2014).

Reenen et al., 2014; Koizumi et al., 2014; Kramers et al., 2014; Safonov et al., 2018b).

GRANITOID MAGMATISM OF THE SOUTHERN MARGINAL ZONE

Geological and Age Relationships with SMZ Granulites

During its metamorphic evolution, SMZ was affected by extensive anatexis (Du Toit et al., 1983; van Reenen et al., 2014; Taylor et al., 2014; Nicoli et al., 2015; Safonov et al., 2018a), but the most intense granitoid magmatism in this zone of the Limpopo Complex occurred during its exhumation and retrogression after 2720–2710 Ma. The most significant magmatic event was the emplacement of the syn-latekinematic Matok diorite–granodiorite–monzogranite pluton at 2686 ± 7 Ma (Fig. 1; Barton et al., 1992; Laurent et al., 2013, 2014; Laurent and Zeh, 2015). According to geochemical data (Laurent et al., 2014), this pluton was produced by magmas derived from a source in the lithospheric mantle and by those derived from crustal material.

SMZ rocks were also affected by small intrusions and dikes of garnet-bearing leucocratic granites, trondhjemites, and granodiorites (Table 1), whose origin is so far disputable. The largest of these granitoid massifs occurs as elongate or equant bodies up to a few hundred meters (Figs. 2a, 2b). The U-Pb zircon age of the granites lies within the range of 2680–2640 Ma (Kreissig et al., 2001; Nicoli et al., 2015; Belyanin et al., 2014). The similarity of the ages of the leucocratic granite intrusions and the Matok pluton indicates that all of them were likely formed by a single or a few roughly simultaneous magmatic events. These events were also coeval with the thrusting of SMZ over the Kaapvaal Craton along the Hout River shear zone (2690–2620 Ma) and with the regional hydration of the granulites at the contact between SMZ and the craton (Fig. 1; van Reenen, 1986; van Reenen et al., 2011; 2014; Smit et al., 2014; Koizumi et al., 2014; Belyanin et al., 2014). Field observations suggest that the leucocratic granitoids were emplaced into already-deformed SMZ granulites and, hence, could not be anyhow related to anatexis of the latter. Similar to the magmas of the Matok pluton (Laurent et al., 2014; Laurent and Zeh, 2015), the magmas of the leucocratic granitoids seem to have been derived from a source outside SMZ. Data on $\delta^{18}O$ of (Vennemann and Smith, 1992; Dubinina et al., 2015) indicate that the leucocratic granitoids were not in equilibrium with the host metapelites of the Bandelierkop Formation, into which the granitoids were emplaced. The $\delta^{13}C$ of the graphite (from –6.52 to –8.65‰) and fluid in fluid inclusions (–4.10 ± 1.2‰) (Safonov et al., 2018b) hosted in minerals of the leucocratic granites are principally different from $\delta^{13}C$ = –15.0 to –12.5‰ of graphite from SMZ metapelites (Vennemann and Smith, 1992), thus confirming that both the magmas and their fluids were derived from external source.

P–T Crystallization Parameters of the Granitoid Magmas

Our samples of the leucocratic granitoids contain relatively few varying mineral assemblages usable for estimating the starting crystallization parameters. However, the cores of plagioclase grains in the trondhjemites often contain antiperthitic lamellas, whose

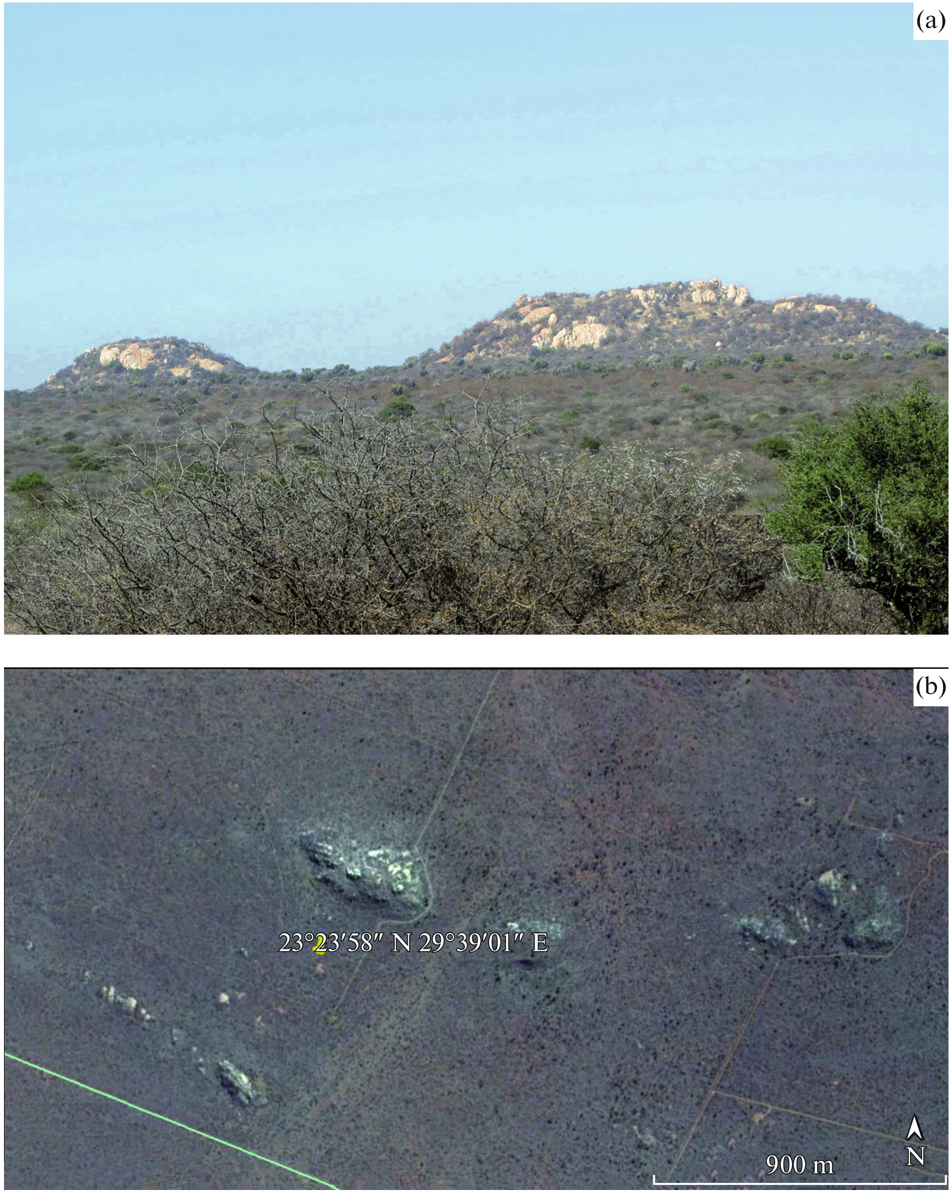

Fig. 2. Bedrock outcrops of the garnet-bearing leucocratic granites in the Southern Marginal Zone of the Limpopo Complex, South Africa. (a) Photo of the Koppieskraal Massif (see Fig. 1). (b) Satellite image (from Google Earth) showing (in map view) the shape and size of the Koppieskraal Massif.

geometries vary from very thin ingrowths to tabular inclusions. Their distribution in the plagioclase crystals indicates that they were formed by the exsolution of plagioclase solid solution but not by metasomatic replacement (Figs. 3a–3d). The granodiorites and granites host perthitic alkali feldspars and mesoperthitic varieties (Figs. 3b, 3c). For example, granodiorites from the Bandelierkop quarry contain perthitic alkali feldspars coexisting with mesoperthites, and hence, these rocks can be classified as hypersolvus granitoids (Fig. 3b). The composition of the alkali feldspars estimated by microprobe scanning allowed us to estimate the crystallization temperatures of the minerals (Figs. 3a–3d): the average temperature values are 850–950°C and reach 1000°C for some of the samples.

Additional information on the temperatures of the granitoids and their crystallization temperatures can be acquired from various inclusions in the garnet. In some of the samples, garnet hosts spinel inclusions (Figs. 4a, 4b). Modeling phase associations of these samples using pseudosections (here and below, the pseudosections were constructed using the PERPLE_X software, version 6.7.7, software; Connolly, 2005) shows that spinel crystallizes within broad ranges of pressures and fluid composition (X_{CO_2}) at

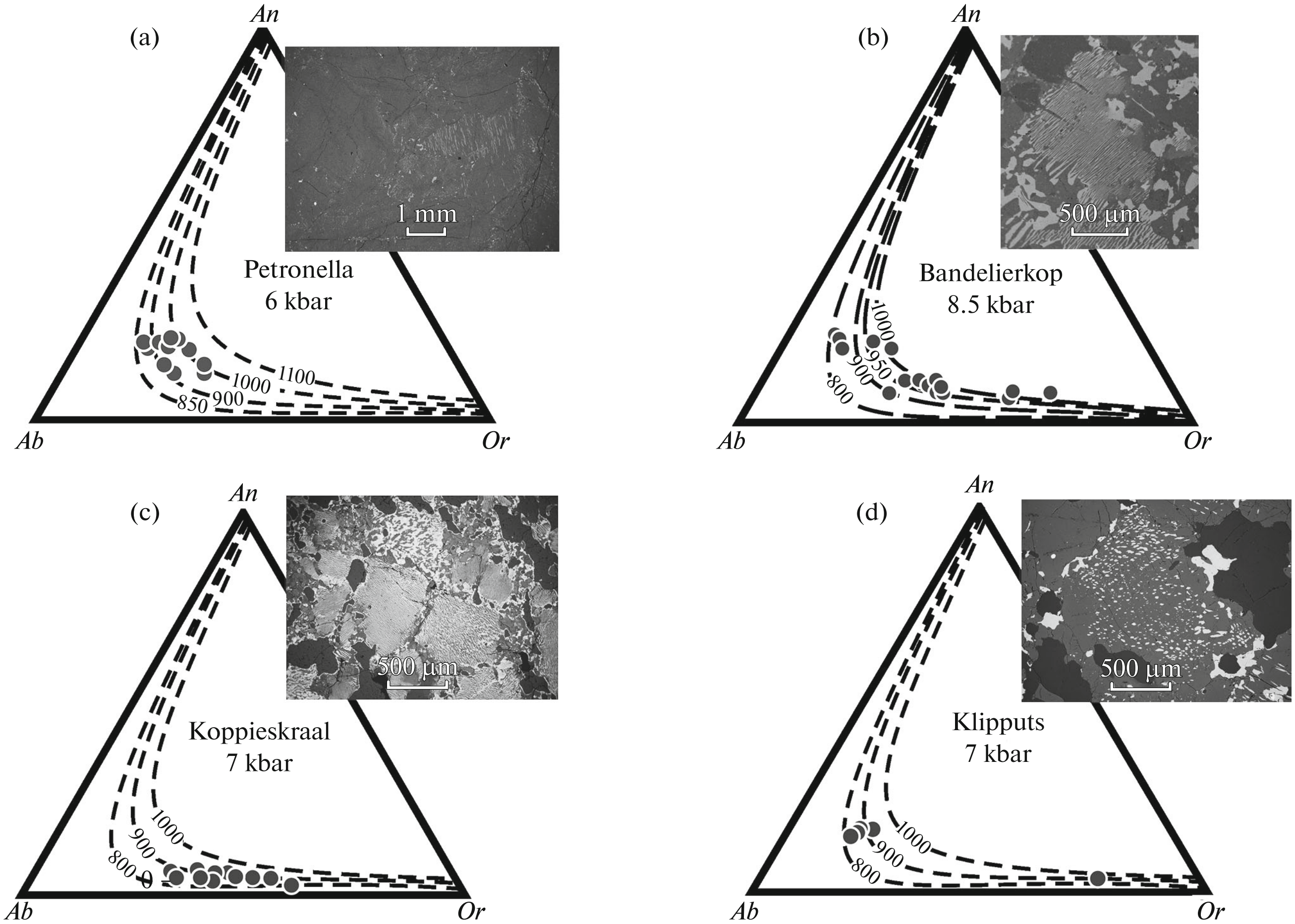

Fig. 3. Reintegrated compositions of feldspars from leucocratic granitoids in (a) Petronella, (b) Bandelierkop, (c) Koppieskraal, and (d) Klipputs. Isotherms are calculated based on the ternary feldspar solid solution model (Elkins and Grove, 1990). BSE images in the insets show the types of exsolution textures in feldspars of the granitoids.

temperatures above 900–950°C but disappears at cooling in the course of garnet-producing reactions (Fig. 5). For example, garnet-hosted polyphase inclusions in trondhjemites from the Petronella locality contain spinel in association with corundum and sillimanite (Fig. 4a) and thus suggest the equilibrium

$$3Spl + 3Sil = Grt + 5Crn, \quad (1)$$

which is shifted to the right-hand side at cooling. The temperatures calculated using Fe–Mg exchange equilibrium between garnet and spinel in this association are 860–890°C (Safonov et al., 2014). Garnet in sillimanite-bearing trondhjemites sampled in the Bandelierkop quarry hosts spinel inclusions together with quartz (Fig. 4b), which points to the equilibrium

$$3Spl + 5Qz = Grt + 2Sil, \quad (2)$$

which also shifts to the right-hand side with a temperature decrease.

The composition of equilibrium garnet and plagioclase in the granitoids reflect equilibrium between these phases and melt at temperatures above 900°C. For example, the crystallization temperature of the association *Grt* + *Pl* + *Qz* + *Rt* found in trondhjemites from the Bandelierkop quarry is 920–950°C, as follows from the pseudosections (Figs. 6a, 6b).

The SMZ leucocratic garnet-bearing granitoids crystallized within a broad pressure range of 6–9 kbar. For example, the crystallization pressures of trondhjemites from the Petronella area were evaluated at 6.3–6.5 kbar (Safonov et al., 2014), and the pressures for the trondhjemites, granodiorites, and granites from the Bandelierkop quarry were 7–9 kbar (Fig. 6b; Safonov et al., 2018b). However, the pseudosections (Figs. 5, 6a) show that the succession of mineral associations produced when the granite magmas cooled only insignificantly depends on pressure: the fields of the phase associations and solidus lines are nearly vertical. Biotite appears at 800–750°C, and muscovite crystallizes at 600–650°C (Figs. 5, 6a). These minerals commonly developed along the margins of garnet and sillimanite grains and replaced relict minerals (orthopyroxene and cordierite) entrained by the granitoids.

The garnet only rarely contains mica inclusions. Nevertheless, trondhjemites in the Petronella area were found out to contain garnet grains of complicated inner structure, which host both polyphase high-temperature inclusions *Spl* + *Sil* + *Crn* in grain cores and polyphase *Bt* + *Sil* + *Qz* inclusions, as well as muscovite inclusions, in grain margins (Fig. 4a). This unique set of inclusions and their distribution in the garnet grains reflect the long-lasting crystallization of the magma, which started at temperatures above 900°C and continued until the temperature dropped to less than 650°C at an insignificant pressure decrease from 6.5 to 5.5 kbar (Safonov et al., 2014).

The cooling of the granitoids is reflected in the weak zoning of the garnet, particularly in the insignificant rimward increase in its X_{Ca}. For example, isopleths in Fig. 6b indicate that cooling from 900–950°C to 700–650°C leads to enrichment of the garnet in grossular by as little as 1–3 mol %.

Fluids in the Granitoid Magmas

CO_2 is the dominant component of fluids that accompanied SMZ granitoid magmas. CO_2 inclusions are remarkably dominant in minerals of the granitoids (Safonov et al., 2014, 2018b). These are usually pseudosecondary inclusions hosted in healed fractures in quartz and garnet (Table 2). However, some inclusions are high-density (1.0–1.1 g/cm^3) primary isolated ones (Table 2). Figures 7a–7c display the types of the CO_2 inclusions hosted in minerals of the trondhjemites and granites from the Bandelierkop quarry (Safonov et al., 2018b). Successive populations of CO_2 inclusions in the granitoids suggest that the granitoid magmas crystallized in the presence of CO_2 fluid starting from the highest temperatures until complete crystallization and ending with subsolidus transformations. The T_m of the CO_2 inclusions in SMZ granitoids (Table 2) are often lower than the melting temperatures of pure CO_2 (–56.6°C) and suggest that the inclusions contain up to 15 mol % CH_4 (see, for example, Kerkhof and Thiéry, 2001), and this is confirmed by the Raman spectra of the inclusions (Safonov et al., 2018b). Methane is a product of later fluid transformations in the inclusions, but its presence indicates that the fluids associated with the granitoid magmas originally consisted not only of CO_2 alone but also contained H_2O, and that the CO_2/H_2O ratio of the fluid varied.

The variations in the CO_2/H_2O ratios in the CO_2–H_2O fluids that accompanied the crystallization of the SMZ leucocratic granitoids are reflected in the mineral assemblages of the rocks, first of all, in the presence (or absence) of hydrous minerals. An example of the first type of the assemblages are garnet- and sillimanite-bearing granite from the Bandelierkop quarry (Safonov et al., 2018b). The granite contains feldspars of various morphological types (Fig. 8a): (1) plagioclase, which in places contains thin antiperthites, (2) mesoperthitic feldspar, which is locally recrystallized into (3) coarse-grained aggregates of potassic feldspar and plagioclase. The rock does not contain biotite. According to the T–X_{CO_2} pseudosection (Fig. 8b), this association can be produced by a granite melt crystallizing in the presence of H_2O–CO_2 fluid with X_{CO_2} above 0.5.

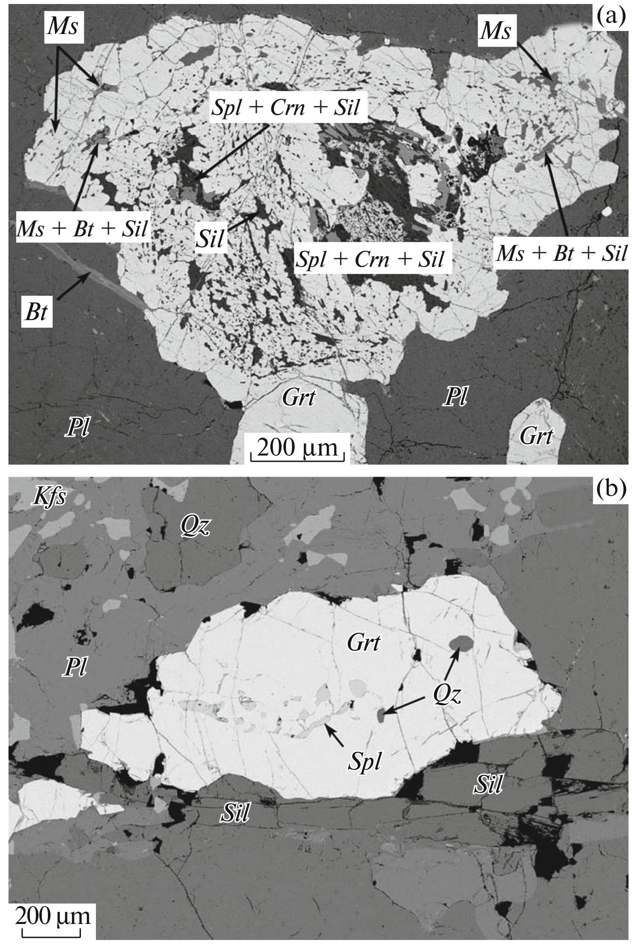

Fig. 4. Spinel inclusions in garnet from the leucocratic granitoids. (a) Polyphase *Spl* + *Crn* + *Sil* in garnet from trondhjemite from the Petronella area (Safonov et al., 2014); the cores of the garnet grains additionally host individual sillimanite inclusions, and closer to the peripheral parts of the garnet grains, they contain polyphase *Ms* + *Bt* + *Sil* inclusions, and the marginal portions of the grains host muscovite inclusions. (b) Spinel and quartz inclusions in granodiorite form the Bandelierkop quarry (Safonov et al., 2018b).

A leading role of CO_2 in the fluids that accompanied the emplacement of the granitoids of the Bandelierkop quarry is confirmed by the presence of graphite in the rocks (Figs. 9a, 9b; Safonov et al., 2018b). The content of this mineral in the rocks is no higher than 1 vol % (Fig. 9a), and its flakes are found in associa-

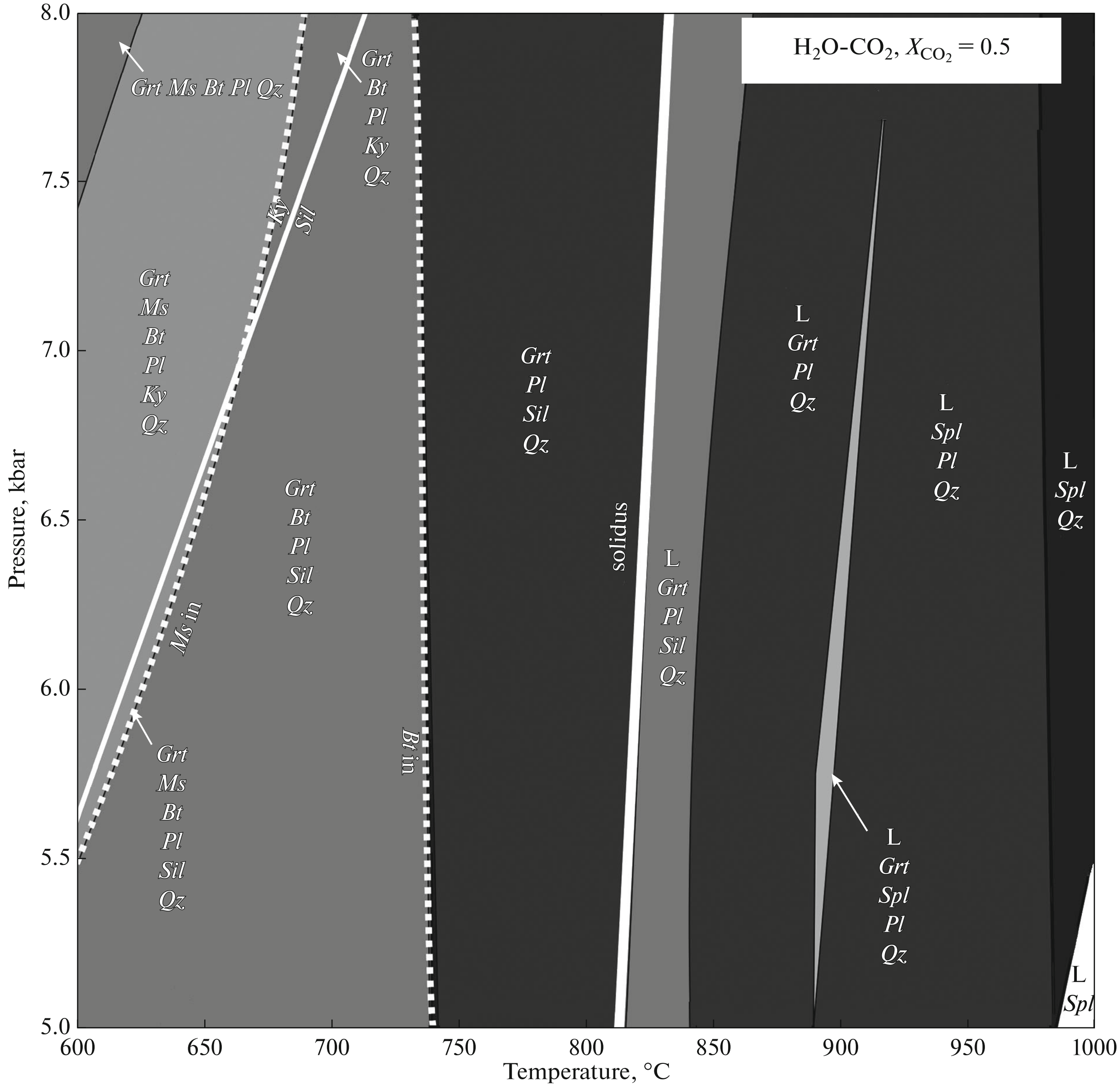

Fig. 5. *P–T* pseudosection for trondhjemite from the Petronella area (PET10, Table 1) showing the succession of mineral associations that crystallized from the trondhjemite magma and subsolidus transformations in the presence of H_2O–CO_2 fluid (X_{CO_2} = 0.5).

tion with garnet, plagioclase, potassic feldspar, sillimanite, and rutile and indicate that the graphite affiliates with the primary mineral assemblage of the granitoids (Fig. 9b). The strong ordering (the only peak G at 1582 cm^{-1} in the Raman spectra) and the unit-cell parameters ($c = 6.7084 \pm 0.0002$ Å and $d_{002} = 3.35347$ Å) indicate that the graphite crystallized at temperatures above 720°C (see, for example, Beyssac et al., 2002).

Information recorded in the mineral assemblages of trondhjemites in the Petronella and Klipputs areas (Fig. 1) is quite different. As was mentioned above, the rocks typically host composite garnet grains with inclusions (Fig. 4a) of mineral associations that crystallized during subisobaric cooling of the magma: from spinel-bearing associations at temperatures above 850–900°C to biotite- and then muscovite-bearing ones at temperatures below 750°C. The trondhjemites contain potassic feldspar (in the form of small exsolution lamellas in the cores of plagioclase grains). According to the T–X_{CO_2} diagram calculated for a representative trondhjemite sample, the sequence of mineral associations could crystallize only at X_{CO_2} < 0.3 (Fig. 10).

Along with H_2O–CO_2 fluids with a variable CO_2/H_2O ratio, the magmas of the SMZ leucocratic

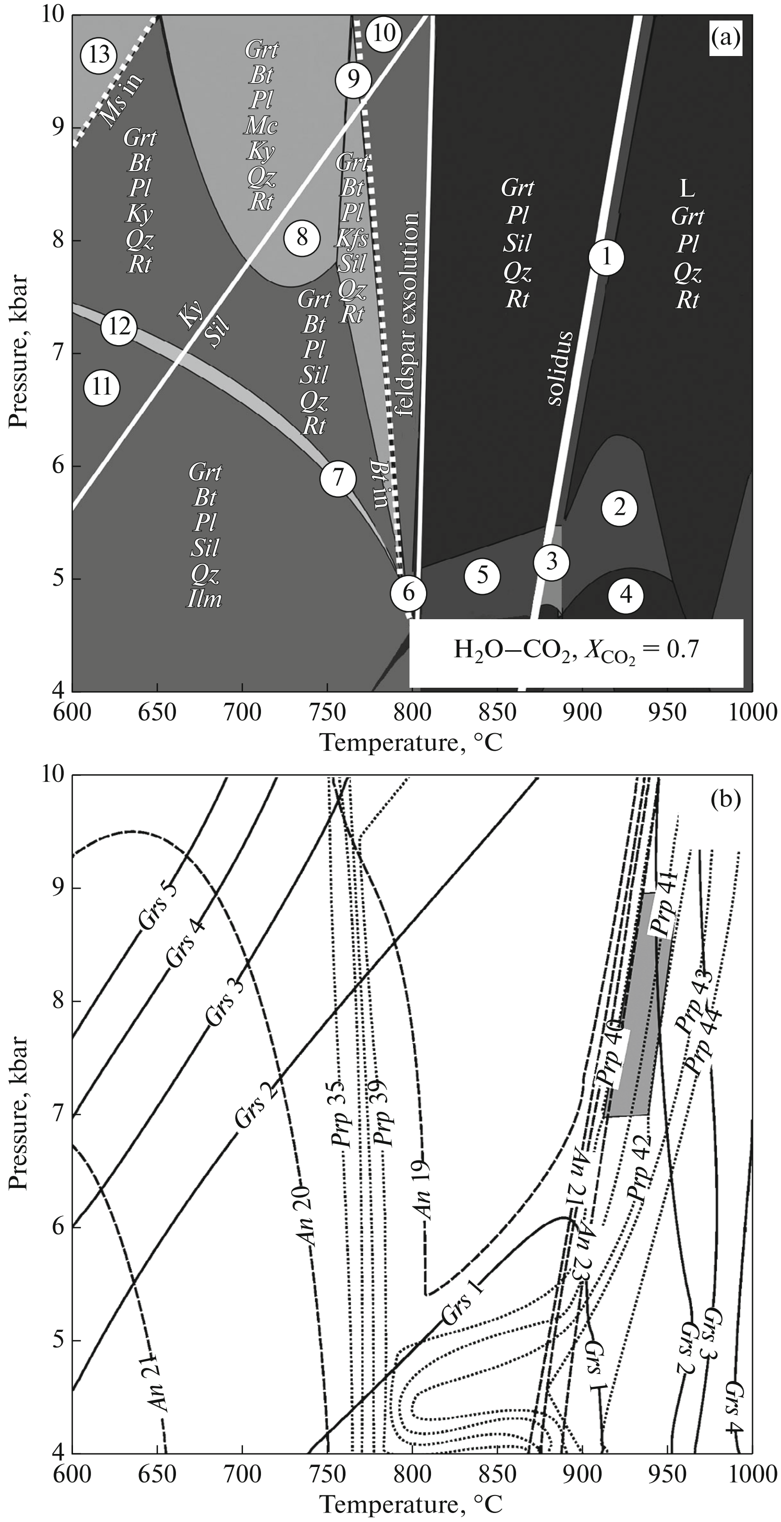

Fig. 6. *P–T* pseudosection for trondhjemite from the Bandelierkop quarry (L14-7-5; Table 1). (a) Mineral associations successively crystallizing from the trondhjemite magma and during subsolidus transformations in the presence of $H_2O–CO_2$ fluid with X_{CO_2} = 0.7. Phase fields: 1. L *Grt Pl Sil Qz Rt*, 2. L *Grt Pl Qz Rt Ilm*, 3. L *Grt Pl Sil Qz Rt Ilm*, 4. L *Grt Pl Qz Ilm*, 5. *Grt Pl Sil Qz Rt Ilm*, 6. *Grt Pl Kfs Sil Qz Rt Ilm*, 7. *Grt Bt Pl Sil Qz Rt Ilm*, 8. *Grt Bt Pl Mc Sil Qz Rt*, 9. *Grt Bt Pl Kfs Ky Qz Rt*, 10. *Grt Pl Kfs Ky Qz Rt*, 11. *Grt Bt Pl Ky Qz Ilm*, 12. *Grt Bt Pl Ky Qz Rt Ilm*, 13. *Grt Ms Bt Pl Ky Qz Rt*. (b) Isopleths of the anorthite component of plagioclase (dashed lines correspond to *An* 19 – *An* 21), pyrope (dashed lines correspond to *Prp* 35–*Prp* 44) and grossular (solid lines correspond to *Grs* 1–*Grs* 5) components of garnet; the gray quadrangle field show the *P–T* ranges of trondhjemite crystallization.

Table 2. Characteristics of CO_2 inclusions in minerals from SMZ granitoids

Granitoid massif	Primary inclusions		Pseudosecondary inclusions	
	T_m, °C	density, g/cm^3	T_m, °C	density, g/cm^3
Bandelierkop quarry	−57.8 to −58.3 (*Qz*)	1.087–1.071 (*Qz*)	−57.3 to −58.7 (*Qz*) −58.9 to −59.2 (*Grt*)	1.06–0.91 (*Qz*) 0.86–0.85 (*Grt*)
	–	–	−57.1 to −58.1 (*Qz*)	1.118–0.627 (*Qz*)
	–	–	−56.8 to −57.3 (*Qz*)	1.122–0.660 (*Qz*)
	–	–	−56.7 to −57.1 (*Qz*)	1.125–0.655 (*Qz*)
Petronella	−57.8 (*Grt*)	1.054–1.020 (*Grt*)	−57.5 to −58.7 (*Grt*) −57.7 to −58.1 (*Qz*)	1.085–0.750 (*Grt*) 1.087–0.719 (*Qz*)
Klipputs	–	–	−56.7 to −61.8 (*Qz*)	1.002–0.617 (*Qz*)
Koppieskraal	–	–	−57.6 to −58.8 (*Qz*)	0.901–0.602 (*Qz*)
Matok	–	–	−57.5 to −57.9 (*Qz*)	0.855–0.632 (*Qz*)
	–	–	−57.1 (*Qz*)	0.945–0.673 (*Qz*)

granitoid carried small portions of H_2O–salt fluids. Relics of these fluids are found as pseudosecondary inclusions that often accompany pseudosecondary CO_2 inclusions (Fig. 11a). These relationships may suggest immiscibility between $H_2O–CO_2$ and H_2O–salt fluid portions (see, for example, Gilbert et al., 1998). The H_2O–salt inclusions start to melt at temperatures from −58 to −53°C and suggest that the solutions contain $CaCl_2$ (these temperatures are close to the eutectic temperatures in the system *ice* + $NaCl \cdot 2H_2O$ + $CaCl_2 \cdot 6H_2O$), and the final melting temperatures are −7 to −17°C and correspond to salt concentrations of 10–20 mol % equiv. NaCl. A mineralogical indicator of interaction between H_2O–salt fluid portions, which accompanied the magmas during their late evolution, are minute veins and rims of potassic feldspar along the boundaries of plagioclase grains (see, for example, Aranovich and Safonov, 2018 and references therein). The late alteration products of the granitoids occasionally contain Cl-bearing apatite and biotite (Safonov et al., 2018b).

Fluid inclusions of similar composition and *P–T* characteristics were found in granitoids and monzonites of the Matok batholith (see, for example, Laurent et al., 2014). The CO_2 inclusions are of the pseudosecondary type, with a relatively low-density (0.945–0.673 g/cm^3) fluid. In the granodiorites, they were found in association with H_2O–salt fluid inclusions whose melting temperatures range from −55 to −53°C, which suggest that the solutions contain $CaCl_2$ and NaCl. An even more complicated composition was detected in quartz-hosted H_2O–salt fluid inclusions in monzogranites the this massif (Fig. 11b): the melting temperatures are −79 to −78.3°C and correspond to solutions of LiCl, $MgCl_2$, $CaCl_2$, and KCl.

THERMAL AND FLUID EFFECTS OF THE GRANITOID INTRUSIONS

Thermal Effects and Local Melting in the Aureoles of the Intrusions

The temperatures of the granitoid melts emplaced into the Southern Marginal Zone of the Limpopo Complex at 2680–2670 Ma, after the exhumation of this complex (at ~2690 Ma; Kreissig et al., 2001), were higher than 900°C. These values are remarkably higher than the temperatures predicted by various authors, based on mineralogical thermobarometry and geochronologic data, for this period of time (see, for example, van Reenen et al., 2011; Nicoli et al., 2014). According to (van Reenen et al., 2011), these temperatures were constrained to the range of 700–750°C, and according to (Nicoli et al., 2014), SMZ rocks had cooled by that time to <650°C. Because of this, the emplaced hot magmas should have inevitably thermally affected the SMZ rocks with the development corresponding mineral assemblages or partial melting.

Some researchers (Tsunogae et al., 2004, Belyanin et al., 2012; Rajesh et al., 2014) present evidence of ultrahigh-temperature (>900°C; Kelsey and Hand, 2015) metamorphism in SMZ. These parameters were determined for the unique mineral associations of the Mg–Al granulites that contain Al-*Opx* + *Sil* + *Qz, Opx* + *Crn,* and *Spl* + *Qz* (Belyanin et al., 2012; Rajesh et al., 2014), and also based on the reintegrated compositions of the antiperthitic plagioclase and the Al concentration in the orthopyroxene in association with garnet (Tsunogae et al., 2004). These authors are prone to believe that the ultrahigh temperatures occurred at the metamorphic peak at 2710–2720 Ma. Indeed, zircons from three samples of the Mg–Al granulites yield ages of 2718–2714 Ma (Rajesh et al., 2014), but these rocks also contain zircons dated at

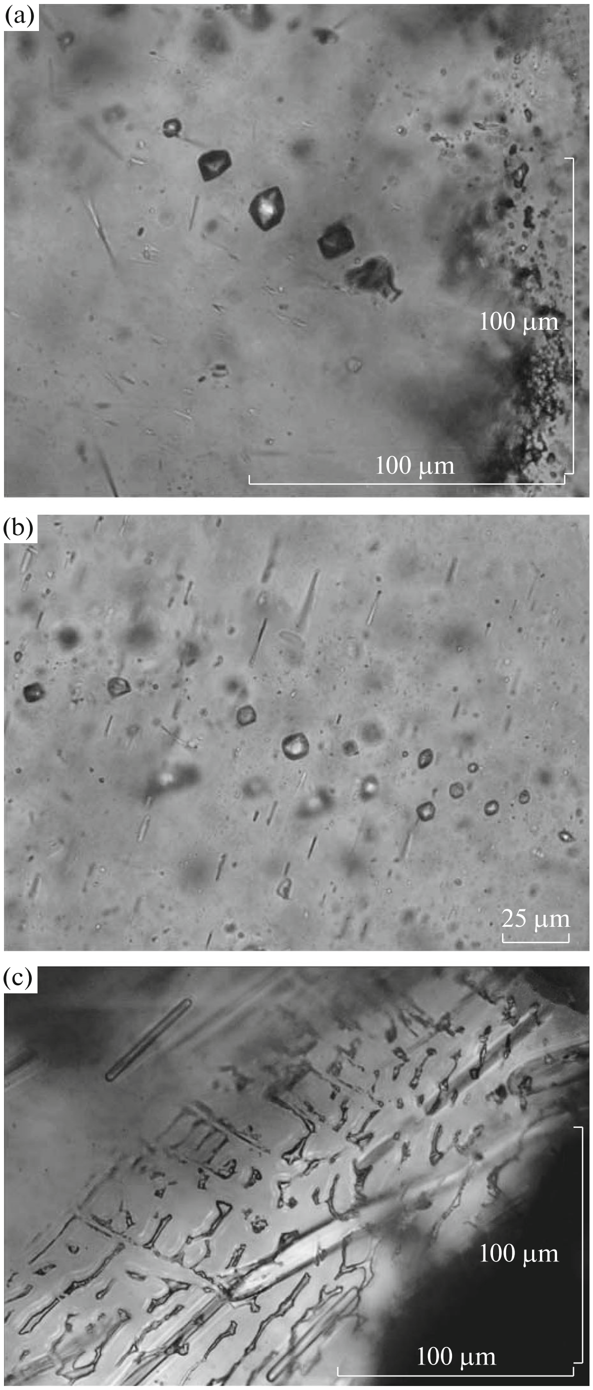

Fig. 7. CO_2 inclusions in granitoids from the Bandelierkop quarry (Safonov et al., 2018b). (a) Isolated group of quartz-hosted primary inclusions. (b) Chain of pseudo-secondary inclusions trapped along a crack in quartz. (c) Wedge-shaped pseudosecondary inclusions in quartz.

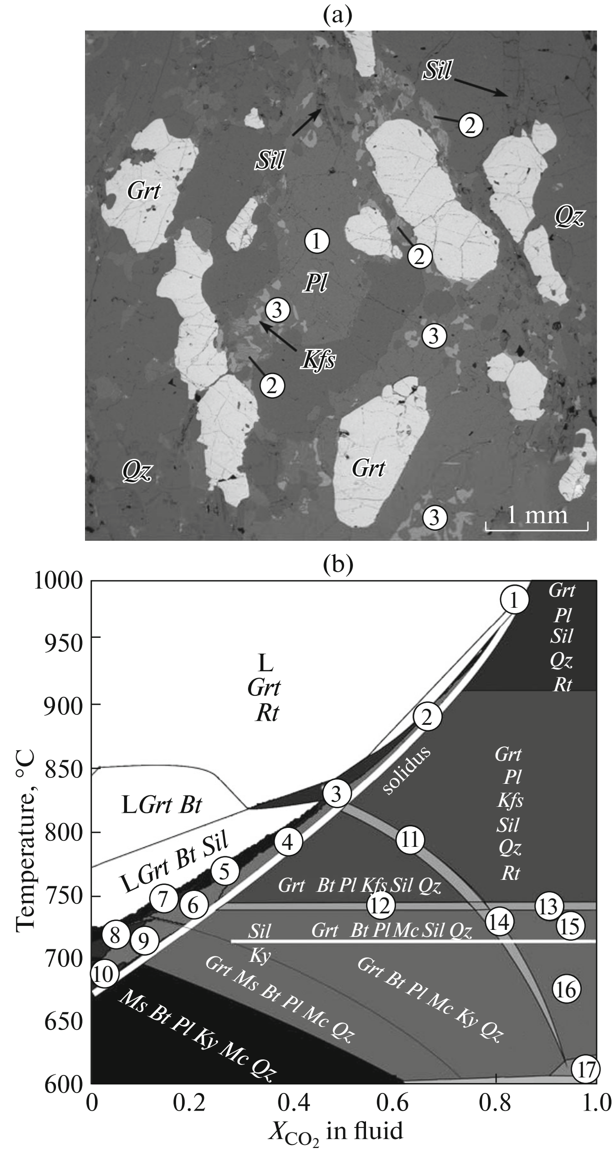

Fig. 8. Mineral associations of the garnet- and sillimanite-bearing granite from the Bandelierkop quarry (L14-7-1; Table 1). (a) Relations between minerals in the granite and morphological types of feldspar in this rock: (1) plagioclase with thin antiperthitic lamellas, (2) mesoperthitic feldspars, (3) recrystallized aggregates of plagioclase and 1kfsp. (b) T–X_{CO_2} pseudosection at a pressure of 8 kbar calculated for the granite composition and showing mineral associations successively crystallizing from the granite magma in equilibrium with H_2O–CO_2 fluid. Phase fields: 1. L *Grt Pl Sil Qz Rt*, 2. L *Grt Pl Kfs Sil Qz Rt*, 3. L *Grt Bt Pl Kfs Sil Qz Rt*, 4. L *Grt Bt Pl Kfs Sil Qz*, 5. L *Grt Bt Pl Sil Qz*, 6. L *Grt Bt Pl Mc Sil Qz*, 7. L *Grt Bt Pl Sil Qz*, 8. L *Grt Mu Bt Pl Qz*, 9. L *Grt Mu Bt Pl Mc Qz*, 10. L *Mu Bt Pl Mc Qz*, 11. *Grt Bt Pl Kfs Sil Qz Rt* 12. *Grt Bt Pl Kfs Mc Qz*, 13. *Grt Pl Kfs Mc Qz*, 14. *Grt Bt Pl Mc Sil Qz Rt*, 15. *Grt Pl Mc Sil Qz Rt*, 16. *Grt Pl Mc Ky Qz Rt*, 17. *Grt Pl Mc Ky Qz Rt Mgs*.

2667–2664 Ma (Rajesh et al., 2014), an age range well correlated with the emplacement age of the leucocratic granitoids (Belyanin et al., 2014).

There are still no other (and stronger) reasons for correlating the origin of the high-temperature Mg–Al granulites with the emplacement of the intrusions. However, we have recently found petrological and geochronological evidence (Safonov et al., 2018a) that the local melting processes of the metapelites were

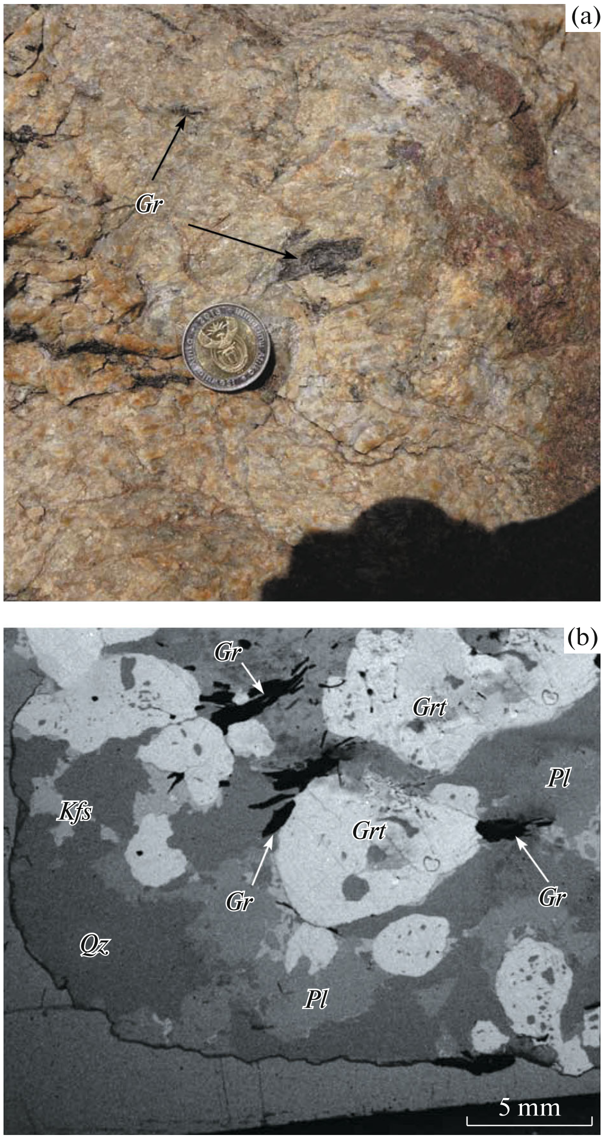

Fig. 9. Graphite in the leucocratic granitoids. (a) Large graphite segregations in the quartz–feldspar matrix of granite from the Bandelierkop quarry (Safonov et al., 2018b) near an assimilated metapelite block; (b) association of graphite with garnet in trondhjemite.

related to the intrusions. These data were derived by studying orthopyroxene–garnet–potassic feldspar patches in metapelites in the Petronella area, which are found in association with the trondhjemite intrusions (Fig. 12a). These patches are equant or ellipsoidal domains 10–100 cm across, which consist of coarse-grained aggregates of feldspar and quartz with large (locally up to 3 cm) subhedral orthopyroxene crystals and smaller (0.5–2 mm) round garnet crystals (Figs. 12a, 12b). The orthopyroxene and garnet proportions of these patches are similar or orthopyroxene strongly dominates over garnet in many of the patches. The patches are also characterized by the strong dominance of perthitic feldspar over plagioclase and quartz, whose proportions are often *Qz/Pl/Kfs* = 20/30/50 (Fig. 12b). The patches are usually not deformed and overprint the foliation of the host rocks but are locally conformable with the foliation. Near contacts with the metapelites, the patches are often surrounded with biotite-rich zones, which are interpreted as melanosome. Along with the typical minerals of the host metapelites (cordierite and biotite), these zones contain garnet and orthopyroxene, whose compositions are close to the compositions of these minerals in the patches (leucosome).

Texturally, the patches exemplify leucosomes typically produced by anatexis in the absence of free fluid phase, or at its insignificant amount (fluid-absent anatexis; Sawyer, 2010). The high content of potassic feldspar and the practically absolute absence of products of high-temperature hydration reactions (biotite) in these patches confirm that they were indeed produced by local melting of biotite-rich metapelites and melt segregation in the absence of external fluid (Safonov et al., 2018a). Relationships between the patches and host metapelites suggest that the melting processes occurred after major metamorphic and deformation events (~2720 Ma) and simultaneously with, or immediately after, the development of foliation and lineation in the host rocks. This conclusion is corroborated by geochronologic data. Zircons and monazites from the patches yield three age ranges (Safonov et al., 2018a): (1) >2900 Ma (zircon cores), which seems to correspond to the deposition of the pelite material of the Bandelierkop Formation (Rajesh et al., 2014; Nicoli et al., 2015), (2) ~2710 Ma (the margins of the zircons and the cores of some of the monazite grains), analogous to the age of the metamorphic peak (Belyanin et al., 2014; Rajesh et al., 2014; Taylor et al., 2014; Nicoli et al., 2015), and (3) 2666 ± 4 (most of the analyzed monazites), which coincides with the emplacement age of the garnet-bearing trondhjemites (2667 ± 9 Ma; Belyanin et al., 2014). The latter age range evidently confirms links between local melting of the metapelites and emplacement of the trondhjemite intrusions (Safonov et al., 2018a). Further support of this conclusion is provided by *P*–*T* data acquired for mineral assemblages in the patches using the pseudosection technique (Figs. 13a, 13b). According to the Al_2O_3 concentration in the orthopyroxene (up to 7.3 wt % at X_{Mg} = 0.60–0.62) in equilibrium with garnet, the crystallization temperature of the mineral assemblage of the patches is estimated at above 900°C at a pressure of 6.5–7.0 kbar (Fig. 13b). These parameters coincide with those of the emplaced trondhjemites. The trondhjemite intrusions provided heat for local melting, and the fluid effect in this process was likely minimal. This follows, for example, from the extreme scarcity of fluid inclusions in minerals from the patches (these are low-density CO_2 inclusions).

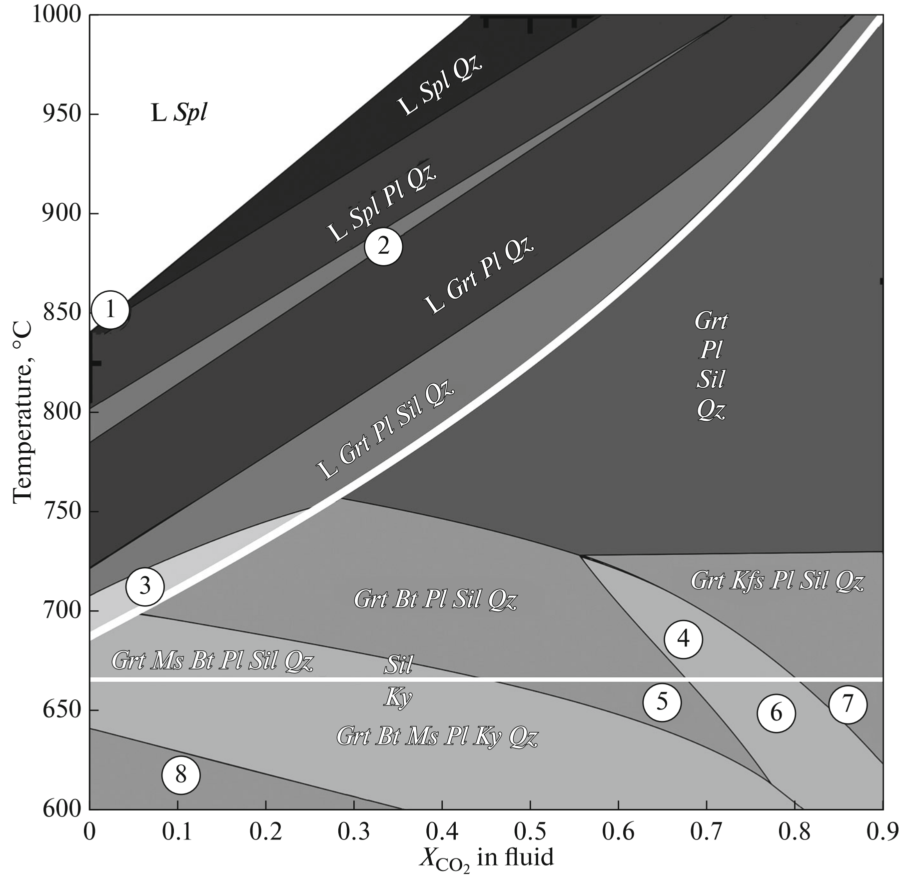

Fig. 10. T–X_{CO_2} pseudosection calculated for a pressure of 6.5 kbar and the composition of trondhjemite from the Petronella area (PET10, Table 1). The pseudosection illustrates the succession of mineral associations crystallizing from the granite magma in equilibrium with H_2O–CO_2 fluid. Fields: 1. L *Spl Pl*, 2. L *Grt Spl Pl Qz*, 3. L *Grt Bt Pl Sil Qz*, 4. *Grt Bt Pl Kfs Sil Qz*, 5. *Grt Bt Pl Ky Qz*, 6. *Grt Bt Pl Kfs Ky Qz*, 7. *Grt Pl Kfs Ky Qz*, 8. *Grt Ms Bt Pl Qz*.

Another example of the local melting of the metapelites under the effect of granitoid intrusions was found in rocks in the Bandelierkop quarry (Figs. 14a, 14b). The melting product was a pegmatoid lens-shaped vein consisting of plagioclase, quartz, biotite, and orthopyroxene whose grains are as large as a few centimeters (Figs. 14a, 14b). In contrast to the patches in the Petronella locality (Figs. 12a, 12b), this vein is devoid of both potassic feldspar (which was found merely as thin lamellas in the plagioclase) and garnet but contains biotite (up to 30 vol %). The biotite is found in two generations (Fig. 14b) of different composition (wt %): (1) X_{Mg} = 0.75–0.76, 3.6–4.4 TiO_2, 0.8–1.1 Cr_2O_3, 0.28–0.36 F for Bt_1 and (2) X_{Mg} = 0.76–0.83, <1 TiO_2, 0.02–0.45 Cr_2O_3, and 0.39–0.49 F for Bt_2. The second-generation biotite coexists with apatite (containing 3.1–4.4 wt % F) and calcite. Considered together with the remarkable variations in the composition of the orthopyroxene (from X_{Mg} = 0.76–0.77 at 6.5–7.1 wt % Al_2O_3 in crystal cores to X_{Mg} = 0.72–0.74 at 4.4–6.5 wt % Al_2O_3 in their margins), these relationships indicate melt crystallization in the vein was associated with enrichment in H_2O, F, and CO_2. The orthopyroxene–biotite equilibrium of the successive generations of these minerals and the reintegrated compositions of the plagioclase cores with potassic feldspar lamellas indicate that melt in the vein started to crystallize at >900°C, and its crystallization terminated at temperatures of about 600–650°C.

In contrast to the orthopyroxene–garnet–potassic feldspar patches in the Petronella area, the above example from the Bandelierkop quarry demonstrates local melting of metapelites in the presence of external H_2O–CO_2 fluid. Relics of this fluid are preserved as both primary and pseudosecondary inclusions in the quartz (as well as such inclusions quartz grains hosted the orthopyroxene). The density of these inclusions varies from 1.037 to 0.895 g/cm^3, and their melting temperatures range from –57.2 to –58.1°C (i.e., the inclusions contain methane). The melting process also evidently involved fluorine, which could be accumu-

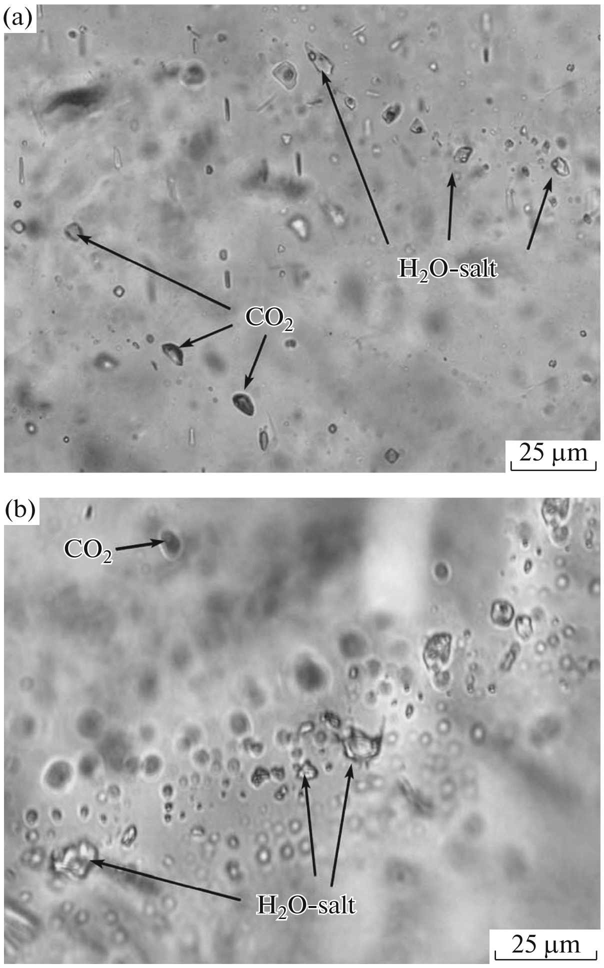

Fig. 11. Pseudosecondary H_2O–salt and CO_2 inclusions in quartz from (a) trondhjemite from the Petronella area (Safonov et al., 2014) and (b) monzogranite from the Matok pluton.

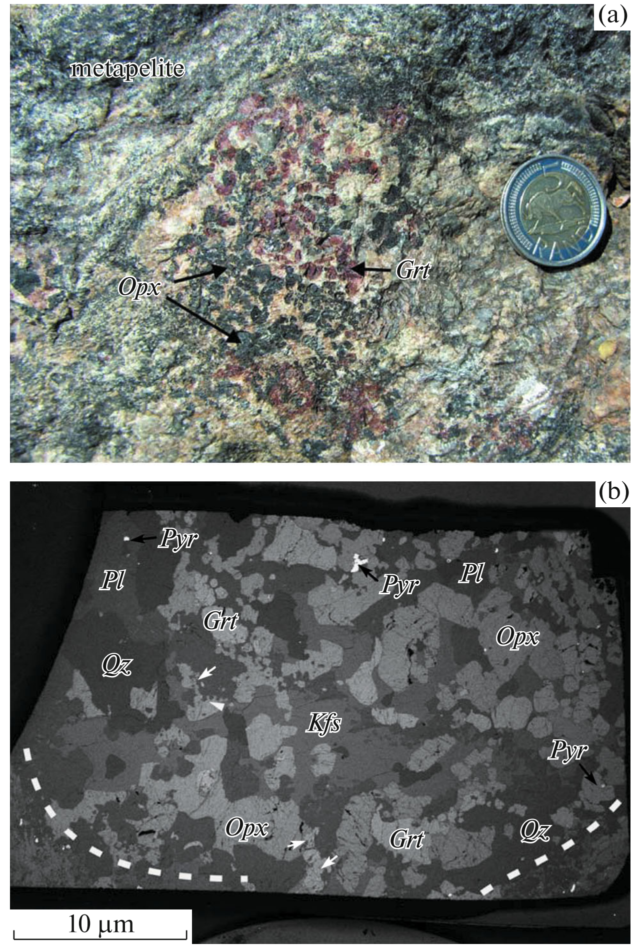

Fig. 12. Orthopyroxene–garnet–potassic feldspar patch in metapelite from the Petronella locality. (a) Relationships with the host metapelite. (b) Relationships between minerals in the rock; dashed lines show the approximate boundaries of the patch.

lated from the melted metapelite and/or brought from outside with the granitoid magmas.

Fluid–Mineral Reactions in the Aureoles of the Granitoid Intrusions

The above example demonstrates that granitoid magmas served as sources of fluid that modified SMZ rocks. This conclusion is not principally new for SMZ (Stevens, 1997; van den Berg and Huizenga, 2001). For example, Stevens (1997) believed that the granitoid magmas of SMZ carried water-rich fluids, which were produced by the anatexis of mica-bearing rocks in SMZ. He also maintained that when the granitoids crystallized, fluids were actively involved in rehydration of the rocks at temperatures <650°C and pressures of 6.0–6.5 kbar and caused, among other things, the establishment of the "orthoamphibole isograd" (Fig. 1). However, our data (Safonov et al., 2014, 2018a, 2018b), which are summarized above, indicate that the fluid brought by the magmas were not pure H_2O but contained CO_2 and salt, with CO_2 sometimes dominating over H_2O, and with the composition of the salt constituent also varying. The conclusion that the fluid of SMZ magmas was of multicomponent is consistent with extensive data (van Reenen and Hollister, 1988; Baker et al., 1992; van den Berg, Huizenga, 2001; Huizenga et al., 2014; van Reenen et al., 2014; Koizumi et al., 2014; Safonov et al., 2014, 2018b) suggesting that H_2O–salt and H_2O–CO_2 fluids participated in the rehydration of SMZ granulites in contact with the Hout River Zone (Fig. 1) at 2660–2670 Ma (Belyanin et al., 2014). The consistency of the composition of the fluids and geochronologic data undoubtedly means that the emplacement of the granitoids and regional-scale interaction with fluids were interrelated.

Variations in the composition of the fluid released from the granitoids are reflected in fluid–mineral reactions in the host granulites (Figs. 15a–15e). Figure 15a

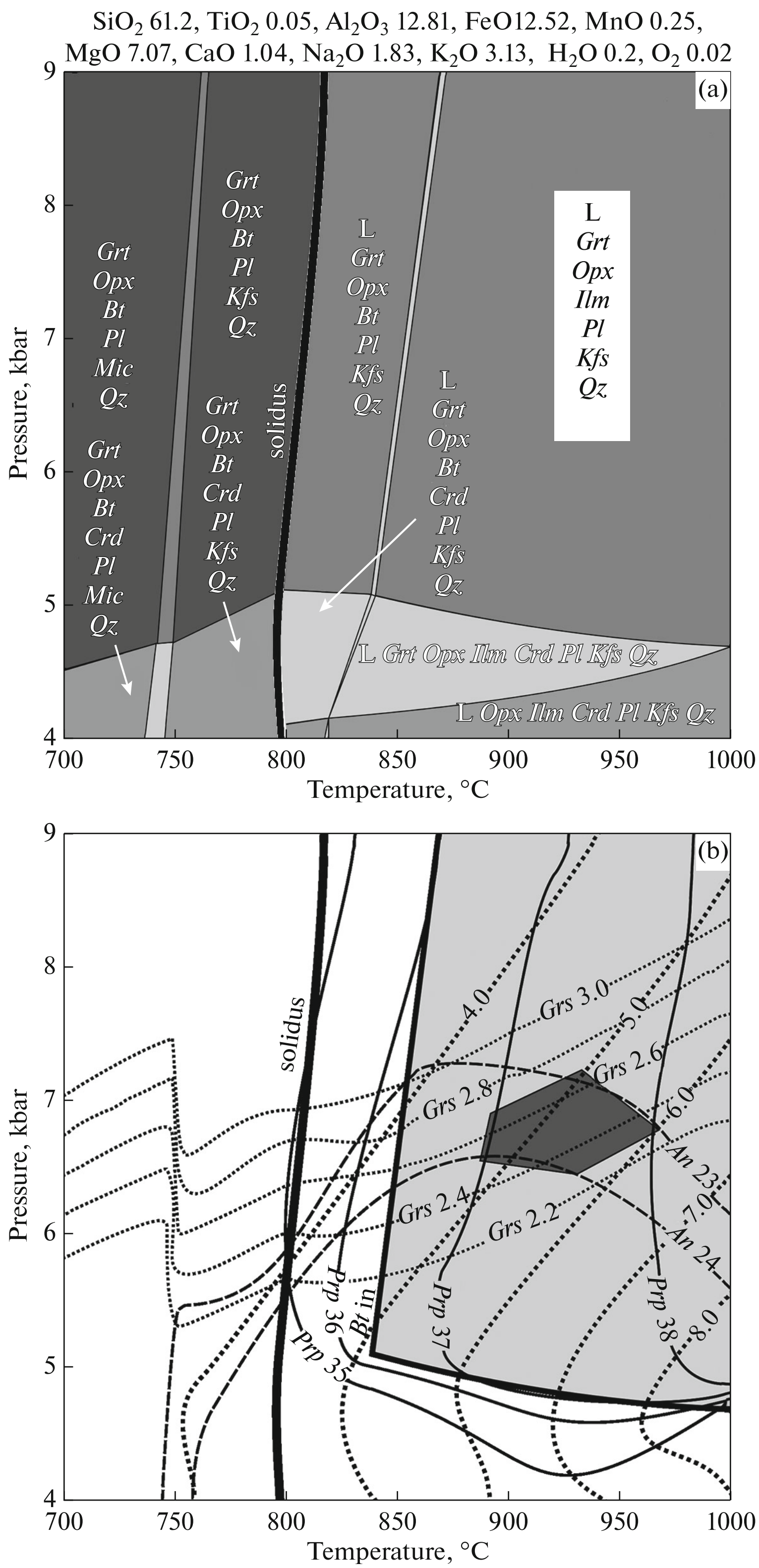

Fig. 13. Phase relations between and compositions of minerals calculated for a representative composition of rock from an orthopyroxene–garnet–potassic feldspar patch in metapelites in the Petronella area (Safonov et al., 2018a). (a) *P–T* pseudosection showing the stability field of the mineral association of the patch L + *Grt* + *Opx* + *Ilm* + *Pl* + *Kfs* + *Qz*. (b) Isopleths of concentration of the pyrope (*Prp* mol %, solid lines) and grossular (*Grs* mol %, dotted lines) components of garnet, the anorthite component of plagioclase (*An* mol %, dashed lines), and Al_2O_3 concentration in orthopyroxene (wt %, heavy solid lines). The dark gray pentagon shows the *P–T* parameters under which the patches were produced.

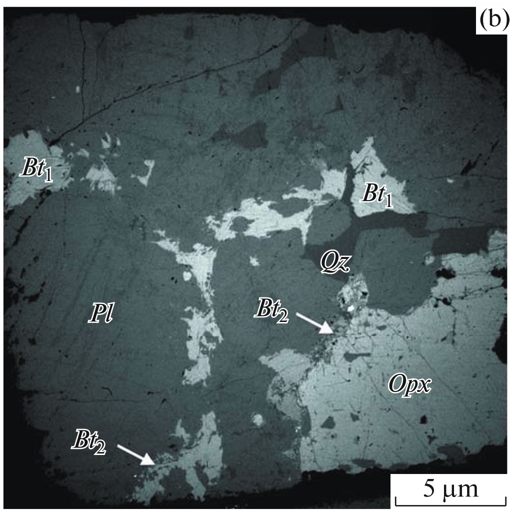

Fig. 14. Pegmatoid vein hosted in metapelite in the Bandelierkop quarry. (a) Photo of the vein, showing its coarse-grained pegmatoid texture. (b) BSE image of a fragment of this vein illustrating the primary mineral association *Opx* + *Bt*$_1$ + *Pl* + *Qz* and later *Bt*$_2$, replacing orthopyroxene and first-generation biotite grains in their margins.

illustrates the association of Fe-bearing dolomite, biotite, graphite, and quartz that replaced orthopyroxene, garnet, and plagioclase in orthopyroxene–garnet metapelite from the Bandelierkop quarry and suggests that the rock interacted with H_2O–CO_2 fluid. Calculations of phase relations for this metapelite (sample SA-4-3; Dubinina et al., 2015) in T-X_{CO_2} diagram at 7 kbar show that the dolomite–ankerite carbonate in association with *Grt* + *Opx* + *Pl* + *Ilm* + *Qz* could be formed at temperatures below 640°C and $X_{CO_2} > 0.5$. Recall that the leucocratic granitoids in the Bandelierkop quarry were associated with CO_2-rich fluid (Fig. 8b). The values of $\delta^{13}C_{PDB} = -5.04‰$ measured in fluid from fluid inclusions in metapelites from the Bandelierkop quarry (Safonov et al., 2018b) are analogous to the isotopic composition of fluid and graphite from the leucocratic granitoids. Unfortunately, we failed to acquire data on the isotopic composition of graphite from the metapelites, but preexisting data in (Vennemann and Smith, 1992) indicate that $\delta^{13}C_{PDB} = -9.3 \pm 0.3‰$ for graphite from the metapelites in contact with the granitoids and $\delta^{13}C_{PDB} = -12.5$ to $-15.2‰$ for graphite from metapelites away from the granitoids and this mineral from the granitoids themselves. This convincingly proves that carbon from more than one source was mixed with the assistance of CO_2 fluid from the intrusions.

Interaction with CO_2 fluid is evident from reactions with sulfides, first of all, with pyrrhotite, a typical mineral of metapelites of the Bandelierkop Formation. The replacement of pyrrhotite by pyrite and Fe–Mg carbonates (Fig. 15b) is described by the reaction

$$2Po + 3CO_2 + 1/2\,O_2 = Py + Sd. \qquad (3)$$

Reactions depicted in Figs. 15a and 15b provide evidence of operation of H_2O–CO_2 fluids. Among the diversity of reactions recording the action of the H_2O–salt constituent of the fluids, it is worth mentioning reactions with cordierite (Figs. 15c, 15d). Typical products of these reactions are Na-bearing gedrite (up to 2.5 wt % Na_2O), plagioclase, and biotite (which is usually poor in TiO_2), which suggest a complex cation composition of the fluid. These mineral phases are commonly found in association with quartz and aluminous phases (sillimanite or kyanite, staurolite) (Fig. 15c). These assemblages can be produced by the following complex reactions involving alkalis and Ca, such as

$$\begin{aligned} &Crd + 7/15\,Na_2O + 1/3\,H_2O \\ &= 1/3\,Na\text{-}Ged + 3/5\,Ab + 6/5\,Sil, \end{aligned} \qquad (4a)$$

$$\begin{aligned} &Crd + 1/6\,Na_2O + 1/3\,H_2O \\ &= 1/3\,Na\text{-}Ged + 3/2\,Qz + 3/2\,Sil, \end{aligned} \qquad (4b)$$

$$\begin{aligned} &Crd + 1/3\,K_2O + 2/3\,H_2O \\ &= 2/3\,Phl + 4/3\,Qz + 10/6\,Sil, \end{aligned} \qquad (4c)$$

$$\begin{aligned} &Crd + 3/2\,CaO + 1/6\,Na_2O + 1/3\,H_2O \\ &= 3/2\,An + 1/3\,Na\text{-}Ged, \end{aligned} \qquad (4d)$$

where Na-*Ged* is the $NaMg_6Al_3Si_6O_{22}(OH)_2$ end member of the amphibole solid solution. In these model reactions, K, Na, and Ca are written in the form of oxides for the sake of better illustration, albeit real fluids contain them in the form of salts, for example, chlorides, as is seen from the composition of the fluid inclusions. Associations of Na-bearing (>3 wt % Na_2O) gedrite and low-Ti (<1 wt % TiO_2) biotite (in associations with feldspars and various aluminous phases) can be formed at interaction between cordierite-bearing metapelite with H_2O–CO_2–KCl and H_2O–CO_2–NaCl fluids at 600 MPa and 850°C, as follows from our experiments (Safonov and Kosova, 2017).

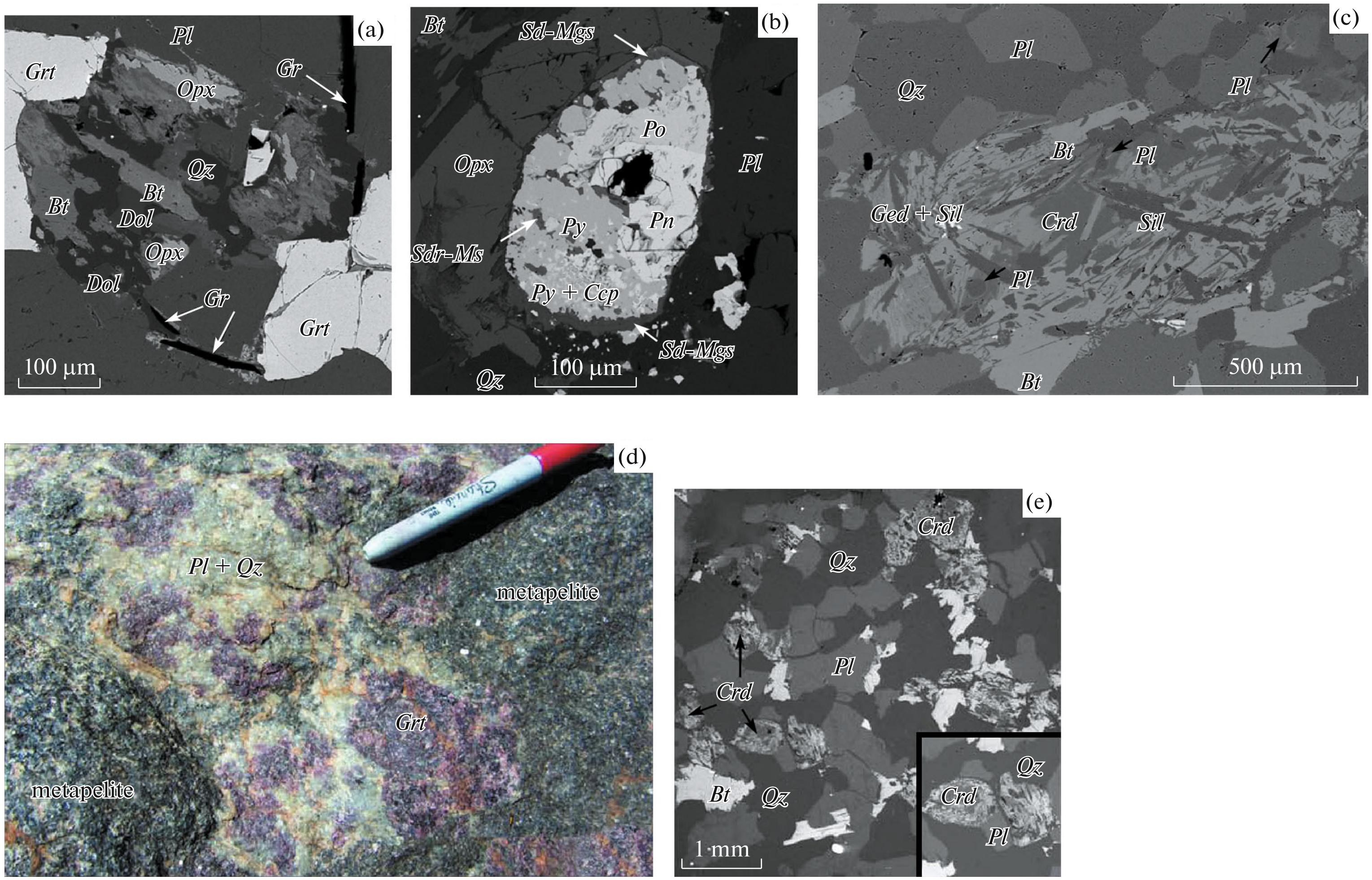

Fig. 15. Reaction textures produced by fluid–mineral interaction in metapelites in the aureoles of granitoid intrusions in SMZ. (a) Association of Fe-bearing dolomite, biotite, graphite, and quartz replacing orthopyroxene, garnet, and plagioclase in orthopyroxene–garnet metapelite from the Bandelierkop quarry. (b) Pyrrhotite replaced by pyrite and siderite–magnesite carbonate in metapelite from the Petronella area. (c) Replacement of cordierite by the assemblage Na-*Ged* + *Bt* + *Sil* + *Pl* + *Qz* in metapelite in the aureole of a trondhjemite intrusion in the Petronella area (Safonov et al., 2014); the replaced cordierite is hosted in a quartz–plagioclase matrix. (d) Garnet–quartz–plagioclase patch in cordierite–biotite metapelite hosting the Matok pluton. (e) The texture of the quartz–plagioclase part of the patch shown in Fig. 15d, with cordierite relics that are replaced by the association Na-*Ged* + *Bt* + *Sil* + *Pl* + *Qz* (see inset).

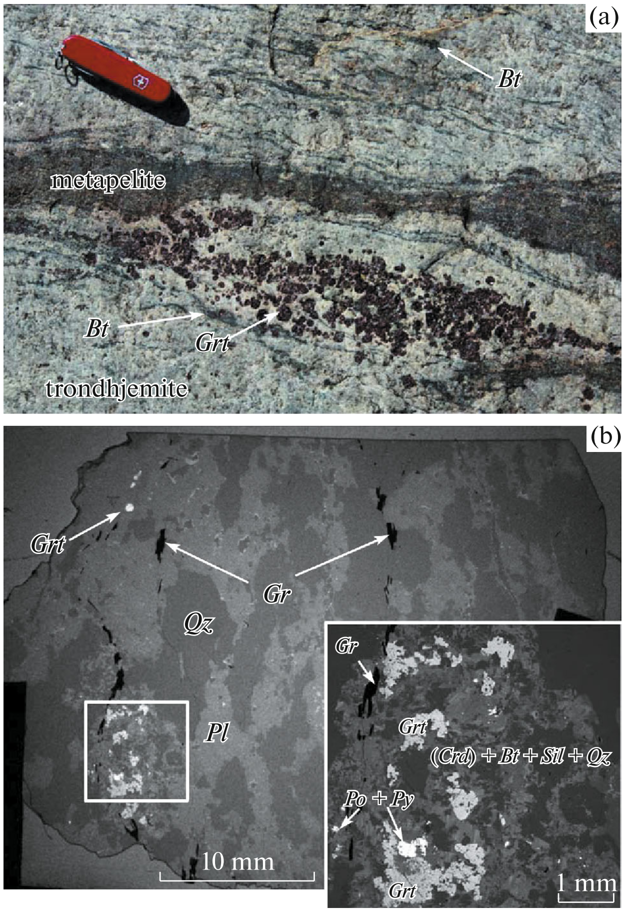

Fig. 16. Assimilation of host gneisses by granitoid magmas. (a) Reaction garnet zone at contact between an attenuated metapelite block and trondhjemite in the Petronella locality (Safonov et al., 2014); biotite lenses in trondhjemite usually host orthopyroxene, cordierite, and garnet relics. (b) Small relict metapelite remnant hosted in trondhjemite and cropping out in the Bandelierkop quarry (Safonov et al., 2018b); the relict block is made up of an aggregate of biotite (which is extensively replaced by chlorite and muscovite), sillimanite, and quartz with garnet, cordierite, and pyrrhotite (replaced by pyrite) relics; graphite flakes developed along the contact between the metapelite block and trondhjemite.

When intensely replaced, the cordierite relics are surrounded by plagioclase–quartz aggregates (Fig. 15c), which developed as leucocratic patches of varying size in the metapelites. An example of such a patch in metapelite in the aureole of the Matok batholith is shown in Figs. 15d–15e. The patch contains newly formed garnet and biotite, whose compositions in association with plagioclase and quartz allowed us to estimate the parameters of their crystallization: 610–640°C and 5.1–6.1 kbar. The garnet is produced by reactions between the initial metapelite and fluid containing Ca and Na salts

$$Crd + 4/3\,\mathrm{CaO} = 4/3\,An + 2/3\,Prp + 1/3\,Qz, \quad (5a)$$

$$Crd + 4/3\,\mathrm{Na_2O} + 5Qz = 8/3\,Ab + 2/3\,Prp. \quad (5b)$$

This is confirmed by the presence of numerous pseudosecondary H_2O–salt inclusions in the quartz. The material of the inclusions starts to melt at temperatures of –55 to –52°C and ends at –18.7 to –15.4°C, which indicates that the solution contains $CaCl_2$, i.e., the inclusions contain 21.7–19.1 wt % equiv. NaCl. As was mentioned above, these H_2O–salt fluids are typical of granitoids of the Matok batholith, which led us to suggest that the fluids that affected the metapelites were genetically related to the fluids of the granitoids.

Temperature at which fluid–mineral reactions proceeded in aureoles around the granitoid intrusions were commonly no higher than 650–700°C and were much lower than the temperatures at which these intrusions started to crystallize. Of course, fluids released from the intrusions also operated at higher temperatures. Evidence of this is provided by the aforementioned pegmatoid vein hosted in metapelites and cropping out in the Bandelierkop quarry (Figs. 14a, 14b). The mineral assemblages of the vein point to an active role of H_2O–CO_2 fluid, which likely originally contained F. However, such examples are rare, and the fluids most actively operated during the late crystallization of the intrusions. This conclusion is consistent with the regularities governing the segregation of fluid phases from crystallizing silicic magmas. Modeling the evolution of the granite melt that contained an H_2O–salt fluid constituent shows that the volume of the released H_2O–salt fluid increased particularly significantly at temperatures close to the solidus (see, for example, Dolejš and Zajacz, 2018). Hence, the relatively low temperatures at which fluids extensively affect the SMZ rocks provide indirect evidence that the fluid–rock interaction was related to the crystallizing granite magmas.

Assimilation of the Host Granulites

Hot granitoid magmas carrying fluid of complex composition are able to assimilate host rocks and thereby modify their own composition. Interaction between the host rocks and granitoid magmas is best seen in some blocks and relict enclaves of these rocks among the granitoids (Figs. 16a, 16b). In a large trondhjemite body in the Petronella area, metapelite blocks are surrounded by zones of large garnet crystals, which also mark the continuations of these blocks within the granitoid body (Safonov et al., 2014). Garnet in these zones hosts numerous inclusions, which reflect the crystallization of the trondhjemites at decreasing temperature (Fig. 4a). The groundmass of the trondhjemites near the metapelite blocks abound in lens-shaped biotite aggregates, which usually contain orthopyroxene and cordierite relics (minerals of the host metapelites). In the Bandelierkop quarry and the granitoid body in the Klipputs area, interaction between trondhjemites and metapelites is inferred from the occurrence of small relict blocks of the metapelites in the granitoids. These relics are commonly strongly hydrated (Fig. 16b), but the aggregates of biotite, sillimanite, and quartz host cordierite relics (Fig. 16b). It is important to mention that if cordierite relics are preserved in the metapelite relict domains, the former are often replaced by garnet growth textures corresponding to the reaction *Crd* = *Grt* + *Sil* + *Qz*. These reaction textures in SMZ metapelites provide compelling mineralogical evidence of the subisobaric cooling of the rocks at pressures of 6.0–6.5 kbar (van Reenen, 1983; Stevens, van Reenen, 1992; Perchuk et al., 1996; Perchuk et al., 2000; Stevens, 1997; Smit et al., 2001, 2014; Taylor et al., 2014; Nicoli et al., 2015; van Reenen et al., 2011, 2014; Safonov et al., 2014). These textures are usually associated with biotite. For example, in one of the metapelite blocks hosted in the granitoids and found in the Bandelierkop quarry, *Grt* + *Sil* + *Qz* reaction textures replacing cordierite contain biotite inclusions, whose X_{Mg} = 0.69–0.72 and which contains 1.5–2.1 wt % Cl (Safonov et al., 2018b). The occurrence of such biotite in the association *Grt* + *Sil* + *Qz* obviously shows that the metapelite block interacted with H_2O–salt fluid, which was released from the granitoid magma at its cooling. According to our data, which are based on the calculation of KCl activity in the fluid (Aranovich, 2017), salt concentration in the fluid may have reached 32 mol % (Safonov et al., 2018b).

Dubinina et al. (2015) have demonstrated that a correlation of $\delta^{18}O$ of leucogranites from the Bandelierkop quarry with their bulk composition (CaO and SiO_2 concentrations) suggests that the granitoid material mixed with the host metapelites of the Bandelierkop Formation. This also follows from the broad variations in the composition of the granitoids, even within a single massif (Table 1), particularly in contact zones. An example is the variations in the composition of leucocratic granitoids in contact with metapelites in the Bandelierkop quarry (Table 1, Figs. 17a–17b). In Figs. 17a and 17b, the “markers” of interaction between the granitoids and metapelites were assumed to be Al_2O_3 and (MgO + FeO), which are major components of the metapelites. Obviously, the variations in the concentrations of these components in the granitoids can be readily obtained by mixing the metapelite and granite material, which contains 75–77 wt % SiO_2 and <2 wt % (MgO + FeO). Such compositions were described in (Taylor et al., 2014) for granites from a small intrusive body that crops out in the quarry. The samples analyzed by Taylor et al. (2014) seem to represent the least contaminated granitoids, whereas the samples from the contact zone are granitoids contaminated with the metapelite material. Garnet (and sillimanite) in samples from the contact zone might have been produced by reactions between the granitoid magma and the host metapelites (similar to what is seen, with an even greater intensity, in trondhjemites from the Petronella area; Fig. 16a) and/or be relict grains borrowed from the metapelites. This hypothesis is confirmed by similarities in the compositional characteristics of some garnets in the granitoid samples (Fig. 18) and garnets in the host metapelites, as well as garnets in relict metapelite remnants in the granitoids (Fig. 16b).

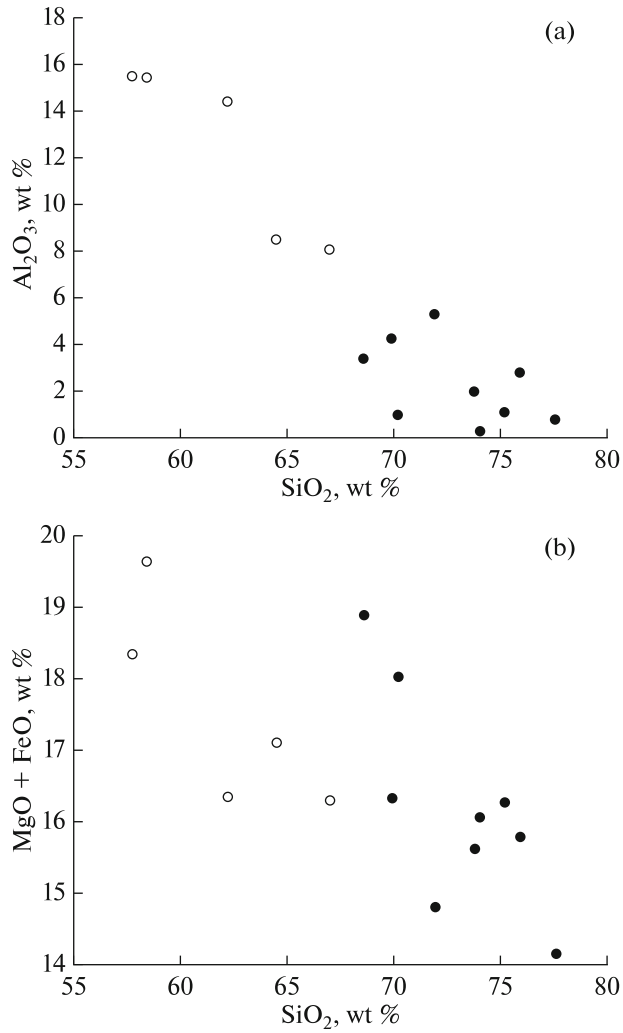

Fig. 17. Variations in the composition of the leucocratic granitoids (solid circles) in the Bandelierkop quarry and their relationships with the compositions of the host metapelite (open circles). (a) Correlations between the SiO_2 and Al_2O_3 concentrations. (b) Correlations between the SiO_2 and (MgO + FeO) concentrations.

In addition to changes in the composition of the melt and mineral assemblages that crystallized in equilibrium with this melt, contamination of the granitoid magmas affected the composition of the fluid phase that accompanied the magmas. This effect was the most significant at contacts between the intrusions and host rocks. For example, in trondhjemites from the Petronella area, garnet replacement by biotite is the most intense near assimilated metapelite blocks

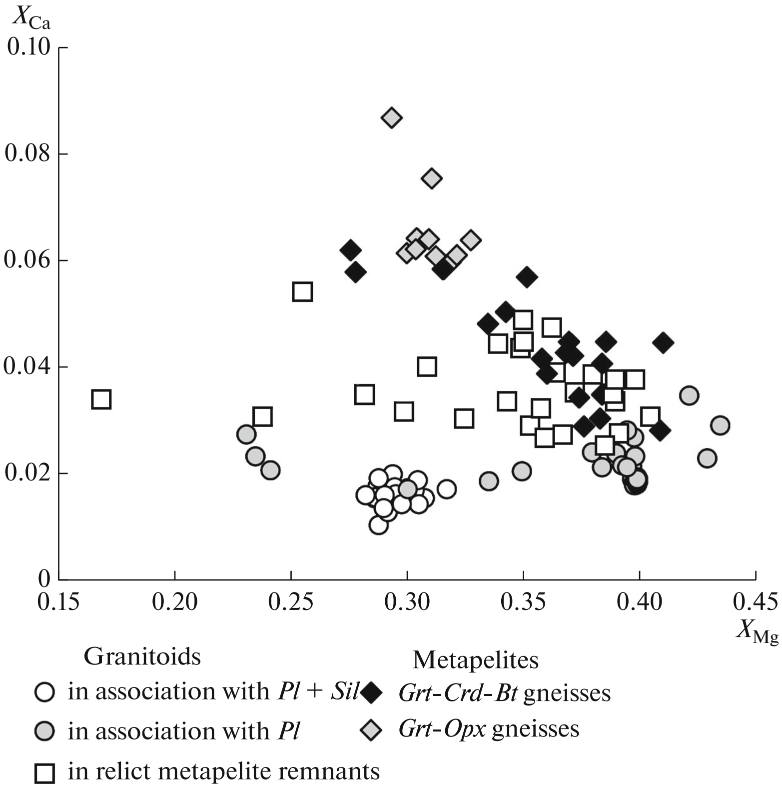

Fig. 18. Comparison of the compositions of garnet from the leucocratic granitoids, host metapelites, and metapelite remnants in the granitoids in the Bandelierkop quarry.

(Fig. 17a). This indicates that the fluid was richer in water where the magma interacted with metapelites. Because of this, variations in the CO_2/H_2O ratio in fluids accompanying the granitoid magmas were likely controlled by assimilation of biotite-bearing rocks by the magmas that carried CO_2 fluid.

A shining manifestation of interaction between fluid of the granitoids with the assimilated material is the crystallization of graphite in granitoids in the Bandelierkop quarry (Figs. 9a, 9b). In graphite and fluid inclusions in these rocks, $\delta^{13}C^{Gr}_{PDB} < \delta^{13}C^{fluid}_{PDB}$ (Safonov et al., 2018b), which corresponds to the near-equilibrium fractionation of carbon isotopes between graphite and CO_2 (see, for example, Polyakov and Kharlashina, 1995) and indicates that the graphite crystallized immediately from CO_2 fluid of the granitoid magmas. We suggest that the graphite crystallized at CO_2 reduction when the magma assimilated the metapelite material, which is rich in sulfides, first of all, pyrrhotite (Fig. 15b)

$$4Po + CO_2 = 2Py + Gr + 2[FeO], \tag{6}$$

where FeO is a component of the silicate melt. In contrast to the host metapelites, the granitoids contain no pyrrhotite, and their dominant sulfide mineral is pyrite, according to reaction (6). The operation of this reaction is confirmed by the low X_{Fe} of garnet in the granitoids as compared to this mineral of the host metapelites and by the crystallization of graphite around relict blocks of pyrrhotite-bearing biotite–cordierite–garnet metapelites in the granites (Fig. 16b). These relationships can be illustrated by reactions involving silicate minerals, sulfides, graphite, and CO_2, such as

$$\begin{aligned} &Po + 1/8\,\text{Fe-}Crd + 1/8\,Qz + 1/4\,CO_2 \\ &= 1/4\,Alm + 1/2\,Py + 1/4\,Gr, \end{aligned} \tag{7a}$$

$$\begin{aligned} &Po + 1/5\,\text{Fe-}Crd + 1/4\,CO_2 \\ &= 3/10\,Alm + 1/2\,Py + 1/4\,Gr + 1/10\,Sil. \end{aligned} \tag{7b}$$

In these reactions, metapelite minerals (cordierite in this instance) are replaced by garnet and sillimanite, which are typical minerals of the leucocratic granitoids.

CONCLUSIONS

Data reviewed and summarized in this paper demonstrate the cumulative thermal and fluid effect of granitoid intrusions on the granulites during their exhumation and retrograde metamorphism. These effects were commonly separated in time in the course of cooling of the intrusions and the separation of fluids from them. This is illustrated by the trondhjemite intrusion in the Petronella area, where the partial melting of host metapelites without any significant influence of fluids was coeval with the emplacement of intrusions, and the fluids operated simultaneously with the later cooling of the intrusions. However, the local thermal and fluid effects were simultaneous, as is demonstrated by the pegmatite vein cropping out in the Bandelierkop quarry (Figs. 14a, 14b). The vein was produced at temperatures above 900°C, with the involvement of H_2O–CO_2 fluid.

Similar thermal–fluid effects of granitoid intrusions and injections were documented in various high-temperature complexes worldwide (see, for example, Jung et al., 1998; Barbosa et al., 2006; Morfin et al., 2013, 2014), the Limpopo Complex among others (Huizenga et al., 2011). In its Central Zone (CZ), the emplacements of multiple granitoid complexes mark metamorphic events in the course of the polymetamorphic evolution of this zone (Perchuk et al., 2008a, 2008b; Huizenga et al., 2011; Brandt et al., 2018; Kröner et al., 2018). Moreover, the emplacement of granitoid massifs in CZ facilitated the exhumation of the complex via the development of numerous dome structures (see, for example, Perchuk et al., 2008b). This highlights the geodynamic effect of granitoid intrusions. In contrast to CZ, granitoid intrusions in SMZ appeared in a single metamorphic cycle. It is pertinent to stress that the time span of magmatic activity in SMZ at 2680–2640 Ma well correlates with the age when abundant granitoids were emplaced in CZ (granitoids Alldays, 2730–2640 Ma; Singelele, 2680–2620 Ma; Verbaard, 2650–2620 Ma, and Avoca, 2650–2630 Ma) (see, for example, Kröner et al., 2018). The geodynamic effect of granitoid intrusions on the exhumation of SMZ and its overthrusting onto the Kaapvaal Craton still awaits its adequate and accurate evaluation.

ACKNOWLEDGMENTS

The authors thank S.G. Skublov (Institute of Precambrian Geology and Geochronology, Russian Academy of Sciences) for constructive criticism and review of the manuscript. This study was financially supported by the Russian Science Foundation (Grant 18-17-00206) in the part devoted to the evolution of Precambrian granulite complexes and the Russian Foundation for Basic Research (project no. 16-05-00266) in the part dealing with the fluid regime of metamorphism.

REFERENCES

Aranovich, L.Ya., The role of brines in high-temperature metamorphism and granitization, *Petrology,* 2017, vol. 25, no. 5, pp. 486–497.

Aranovich, L.Y. and Safonov, O.G., *Halogens in high-grade metamorphism, The role of Halogens in Terrestrial and Extraterrestrial Geochemical Processes,* Harlov, D.E. and Aranovich, L.Y., Eds., (Springer, 2018).

Baker, J., van Reenen, D.D., Van Schalkwyk, J.F., et al., Constraints on the composition of fluids involved in retrograde anthophyllite formation in the Limpopo Belt, South Africa, *Precambrian Res.,* 1992, vol. 55, pp. 327–336.

Barbosa, J., Nicollet, C., Leite, C., et al., Hercynite–quartz-bearing granulites from Brejoes dome area, Jequie Block, Bahia, Brazil: influence of charnockite intrusion on granulite facies metamorphism, *Lithos,* 2006, vol. 92, pp. 537–556.

Barton, J.M., Doig, R., Smith, C.B., et al., Isotopic and REE characteristics of the intrusive charnoenderbite and enderbite geographically associated with the Matok pluton, Limpopo Belt, Southern Africa, *Precambrian Res.,* 1992, vol. 55, pp. 451–567.

Belyanin, G.A., Rajesh, H.M., Sajeev, K., et al., Ultrahigh-temperature metamorphism from an unusual corundum + orthopyroxene intergrowth bearing Al–Mg granulite from the Southern Marginal Zone, Limpopo Complex, South Africa, *Contrib. Mineral. Petrol.,* 2012, vol. 164, pp. 457–475.

Belyanin, G.A., Kramers, J.D., Vorster, C., et al., The timing of successive fluid events in the Southern Marginal Zone of the Limpopo Complex, South Africa: constraints from ^{40}Ar–^{39}Ar geochronology, *Precambrian Res.,* 2014, vol. 254, pp. 169–193.

Beyssac, O., Goffe, B., Chopin, C., et al., Raman spectra of carbonaceous material in metasediments: a new geothermometer, *J. Metamorph. Geol.,* 2002, vol. 20, pp. 859–871.

Blenkinsop, T.G., Archean magmatic granulites, diapirism, and Proterozoic reworking in the Northern Marginal Zone of the Limpopo Belt, *Geol. Soc. Amer. Mem.,* 2011, vol. 207, pp. 245–267.

Brandt, S., Klemd, R., Li, Q. et al., Pressure–temperature evolution during two granulite-facies metamorphic events (2.62 and 2.02 Ga) in rocks from the Central Zone of the Limpopo Belt, South Africa, *Precambrian Res.,* 2018 (in press). https://doi.org/10.1016/j.precamres.2018.03.002.

Brown, M., *Melt extraction from lower continental crust of orogens: the field evidence, Evolution and Differentiation of the Continental Crust, Brown, M. and Rushmer, T.,* Cambridge: University Press, 2006.

Brown, M., Granite: from genesis to emplacement, *GSA Bull.,* 2013, vol. 125, pp. 1079–1113.

Clemens, J.D., *The granulite–granite connection," Granulites and Crustal Evolution*, Ansterdam: Springer, 1990.

Condie, K.C., Belousova, E., Griffin, W.L., et al., Granitoid events in space and time: constraints from igneous and detrital zircon age spectra, *Gondwana Res,* 2009, vol. 15, pp. 228–242.

Connolly, J.A.D., Computation of phase equilibria by linear programming: a tool for geodynamic modeling and its application to subduction zone decarbonation, *Earth Planet. Sci. Lett.,* 2005, vol. 236, pp. 524–541.

Dolejs, D. and Zajacz, Z., *Halogens in silicic magmas and their hydrothermal systems, The Role of Halogens in Terrestrial and Extraterrestrial Geochemical Processes,* Harlov, D.E. and Aranovich, L.Y., Eds., Springer Geochemistry, 2018.

Dubinina, E.O., Aranovich, L.Y., van Reenen, D.D., et al., Involvement of fluids in the metamorphic processes within different zones of the Southern Marginal Zone of the Limpopo Complex, South Africa: an oxygen isotope perspective, *Precambrian Res.,* 2015, vol. 256, pp. 48–61.

Du Toit, M.C., Van Reenen, D.D., and Roering, C., Some aspects of the geology, structure and metamorphism of the Southern Marginal Zone of the Limpopo metamorphic complex, *Spec. Publ. Geol. Soc. South Africa,* 1983, vol. 8, pp. 121–142.

Elkins, L.T. and Grove, T.L., Ternary feldspar experiments and thermodynamic models, *Am. Mineral.,* 1990, vol. 75, pp. 544–559.

Gilbert, F., Guillaume, D., and Laporte, D., Importance of fluid immiscibility in the H_2O–NaCl–CO_2 system and selective CO_2 entrapment in granulites: experimental phase diagram at 5–7 kbar, 900°C and wetting textures, *Eur. J. Mineral.,* 1998, vol. 10, pp. 1109–1123.

Halla, J., Whitehouse, M.J., Ahmad, T., et al., Archean granitoids: an overview and significance from a tectonic perspective, *Geol. Soc. London: Spec. Publ.,* 2017, vol. 449, pp. 1–18.

Huizenga, J.-M., Perchuk, L.L., van Reenen, D.D., et al., Granite emplacement and the retrograde *PT*–fluid evolution of Neoarchean granulites from the central zone of the Limpopo Complex, *Geol. Soc. Amer. Mem.,* 2011, vol. 207, pp. 125–142.

Huizenga, J.-M., Van Reenen, D., and Touret, J.L., Fluid–rock interaction in retrograde granulites of the Southern Marginal Zone, Limpopo high grade terrain, South Africa, *Geosci. Front.,* 2014, vol. 5, pp. 673–682.

Jung, S., Mezger, K., Masberg, P., et al., Petrology of an intrusion-related high-grade migmatite: implications for partial melting of metasedimentary rocks and leucosome-forming processes, *J. Metamorph. Geol.,* 1998, vol. 16, pp. 425–445.

Kelsey, D.E. and Hand, M., On ultrahigh temperature crustal metamorphism: phase equilibria, trace element thermometry, bulk composition, heat sources, timescales and tectonic settings, *Geosci. Front.,* 2015, vol. 6, pp. 311–356.

Kemp, A.I.S. and Hawkesworth, C.J., *Granitic perspectives on the generation and secular evolution of the continental crust, Treatise on Geochemistry,* Rudnick R.L., Eds., Oxford: Elsevier–Pergamon, 2003, pp. 349–410.

Koizumi, T., Tsunogae, T., and van Reenen, D.D., Fluid evolution of partially retrogressed pelitic granulite from the Southern Marginal Zone of the Neoarchean Limpopo Complex, South Africa: evidence from phase equilibrium modeling, *Precambrian Res.,* 2014, vol. 253, pp. 146–156.

Kramers, J.D., McCourt, S., Roering, C., et al., Tectonic models proposed for the Limpopo Complex: mutual compatibilities and constraints, *Geol. Soc. Amer. Mem.,* 2011, vol. 207, pp. 311–324.

Kramers, J.D., Henzen, M., and Steidle, L., Greenstone belts at the northernmost edge of the Kaapvaal Craton: timing of tectonic events and a possible crustal fluid source, *Precambrian Res.,* 2014, vol. 253, pp. 96–113.

Kreissig, K., Nagler, T.F., Kramers, J.D., et al., An isotopic and geochemical study of the northern Kaapvaal Craton and the Southern Marginal Zone of the Limpopo Belt: are they juxtaposed terranes?, *Lithos,* 2000, vol. 50, pp. 1–25.

Kreissig, K., Holzer, L., and Frei, R., Geochronology of the Hout River shear zone and the metamorphism in the Southern Marginal Zone of the Limpopo Belt, Southern Africa, *Precambrian Res.,* 2001, vol. 109, pp. 145–173.

Kröner, A., Brandl, G., Brandt, S., et al., Geochronological evidence for Archaean and Palaeoproterozoic polymetamorphism in the central zone of the Limpopo Belt, South Africa, *Precambrian Res.,* 2018, vol. 310, pp. 320–347.

Laurent, O., Paquette, J.L., Martin, H., et al., LA-ICP-MS dating of zircons from Meso- and Neoarchean granitoids of the Pietersburg block (South Africa): crustal evolution at the northern margin of the Kaapvaal Craton, *Precambrian Res.,* 2013, vol. 230, pp. 209–226.

Laurent, O., Rapopo, M., Stevens, G., et al., Contrasting petrogenesis of Mg–K and Fe–K granitoids and implications for post-collisional magmatism: case study from the late-Archean Matok pluton (Pietersburg Block, South Africa), *Lithos,* 2014, vol. 196–197, pp. 131–149.

Laurent, O. and Zeh, A., A linear Hf isotope–age array despite different granitoid sources and complex Archean geodynamics: example from the Pietersburg Block (South Africa), *Earth Planet. Sci. Lett.,* 2015, vol. 430, pp. 326–338.

Morfin, S., Sawyer, E.W., and Bandyayera, D., Large volumes of anatectic melt retained in granulite facies migmatites: an injection complex in Northern Quebec, *Lithos,* 2013, vol. 168–169, pp. 200–218.

Morfin, S., Sawyer, E.W., and Bandyayera, D., The geochemical signature of a felsic injection complex in the continental crust: Opinaca Subprovince, Quebec, *Lithos,* 2014, vol. 196–197, pp. 339–355.

Nicoli, G., Stevens, G., Moyen, J.-F., et al., Rapid evolution from sediment to anatectic granulite in an Archean continental collision zone: the example of the Bandelierkop Formation metapelites, South Marginal Zone, Limpopo Belt, South Africa, *J. Metamorph. Geol.,* 2015, vol. 33, pp. 177–202.

Perchuk, L.L., van Reenen, D.D., Smit, C.A., et al., Role of granite intrusions for the formation of ring structures in granulite complexes: examples from the Limpopo Belt, South Africa, *Petrology,* 2008, vol. 16, pp. 652–678.

Perchuk, L.L., Gerya, T.V., van Rinen, et al., The Limpopo metamorphic belt, South Africa: 2. Decompression and cooling regimes of granulites and adjacent rocks of the Kaapvaal Craton, *Petrology,* 1996, vol. 4, no. 6, 571–599.

Perchuk, L.L., Gerya, T.V., van Reenen, D.D., et al., Comparative petrology and metamorphic evolution of the Limpopo (South Africa) and Lapland (Fennoscandia) high grade terrains, *Mineral. Petrol.,* 2000, vol. 69, pp. 69–107.

Perchuk, L.L., Van Reenen, D.D., Varlamov, D.A., et al., *P–t* record of two high-grade metamorphic events in the central zone of the Limpopo Complex, South Africa, *Lithos,* 2008, vol. 103, pp. 70–105.

Polyakov, V.B. and Kharlashina, N.N., The use of heat capacity data to calculate carbon isotope fractionation between graphite, diamond, and carbon dioxide: a new approach, *Geochim. Cosmochim. Acta,* 1995, vol. 59, pp. 2561–2572.

Rajesh, H.M., Santosh, M., Wan, D., et al., Ultrahigh temperature granulites and magnesian charnockites: evidence for Neoarchean accretion along the northern margin of the Kaapvaal Craton, *Precambrian Res.,* 2014, vol. 246, pp. 150–159.

Retief, E.A., Compston, W., Armstrong, R.A., et al., Characteristics and preliminary U–Pb ages of zircons from Limpopo Belt lithologies, *Extended Abstracts, Limpopo Workshop. Rand Afrikaans University, Johannesburg, South Africa,* 1990, pp. 95–99.

Safonov, O.G., Yapaskurt, V.O., Elburg, M. et al., *P–T* conditions, mechanism and timing of the localized melting of metapelites from the Petronella shear-zone and relationships with granite intrusions in the Southern Marginal Zone of the Limpopo Belt, South Africa, *J. Petrol,* 2018a, vol. 59, no. 4, pp. 695–734. doi 10.1093/petrology/egy052

Safonov, O.G. and Kosova, S.A., Fluid–mineral reactions and melting of orthopyroxene–cordierite–biotite gneiss in the presence of H_2O-CO_2-NaCl and H_2O-CO_2-KCl fluids under parameters of granulite-facies metamorphism, *Petrology,* 2017, vol. 25, no. 5, pp. 458–485.

Safonov, O.G., Tatarinova, D.S., van Reenen, D.D., et al., Fluid-assisted interaction of peraluminous metapelites with trondhjemitic magma within the Petronella shear-zone, Limpopo Complex, South Africa, *Precambrian Res.,* 2014, vol. 253, pp. 114–145.

Safonov, O.G., Reutsky, V.N., Varlamov, D.A., et al., Composition and source of fluids in high-temperature graphite-bearing granitoids associated with granulites: examples from the Southern Marginal Zone, Limpopo Complex, South Africa, *Gondwana Res.,* 2018b, vol. 60, pp. 129–152.

Sawyer, E.W., Migmatites formed by water-fluxed partial melting of a leucogranodiorite protolith: microstructures in the residual rocks and source of the fluid, *Lithos,* 2010, vol. 116, pp. 273–286.

Sawyer, E.W., Cesare, B., and Brown, M., When the continental crust melts, *Elements,* 2011, vol. 7, pp. 229–234.

Smit, C.A. and van Reenen, D.D., Deep crustal shear zone, high-grade tectonites, and associated metasomatic alteration in the Limpopo Belt, South Africa: implications for deep crustal processes, *J. Geol.,* 1997, vol. 106, pp. 37–57.

Smit, C.A., Van Reenen, D.D., Gerya, T.V., et al., *P–T* conditions of decompression of the Limpopo high-grade terrain: record from shear zones, *J. Metamorph. Geol.,* 2001, vol. 19, pp. 249–268.

Smit, C.A., van Reenen, D.D., Roering, C., et al., Neoarchean to Paleoproterozoic evolution of the polymetamorphic central zone of the Limpopo Complex, *Geol. Soc. Amer. Mem.,* 2011, vol. 207, pp. 213–244.

Smit, C.A., van Reenen, D.D., and Roering, C., Role of fluids in the exhumation of the Southern Marginal Zone of the Limpopo Complex, South Africa, *Precambrian Res.,* 2014, vol. 253, pp. 81–95.

Stevens, G. and van Reenen, D.D., Partial melting and the origin of metapelitic granulites in the Southern Marginal Zone of the Limpopo Belt, South Africa, *Precambrian Res.,* 1992, vol. 55, pp. 303–319.

Stevens, G., Melting, carbonic fluids and water recycling in the deep crust: an example from the Limpopo Belt, South Africa, *J. Metamorph. Geol.,* 1997, vol. 15, pp. 141–154.

Taylor, J., Nicoli, G., Stevens, G., et al., The process that control leucosome composition in metasedimentary granulites: perspectives from the Southern Marginal Zone, Limpopo Belt, South Africa, *J. Metamorph. Geol.,* 2014, vol. 32, pp. 713–742.

Tsunogae, T., Miyano, T., van Reenen, D.D., et al., Ultrahigh-temperature metamorphism of the Southern Marginal Zone of the Archean Limpopo Belt, South Africa, *J. Mineral. Petrol. Sci.,* 2004, vol. 99, pp. 213–224.

van den Berg, R. and Huizenga, J.-M., Fluids in granulites of the Southern Marginal Zone of the Limpopo Belt, South Africa, *Contrib. Mineral. Petrol.*, 2001, vol. 141, pp. 529–545.

van den Kerkhof, A.M. and Thiery, R., Carbonic inclusions, *Lithos,* 2001, vol. 55, pp. 49–68.

van Reenen, D.D., Cordierite + garnet + hypersthene + biotite-bearing assemblages as a function of changing metamorphic conditions in the Southern Marginal Zone of the Limpopo metamorphic complex, South Africa, *Geol. Soc. South Africa. Spec. Publ.,* 1983, vol. 8, pp. 143–167.

van Reenen, D.D., Hydration of cordierite and hypersthene and a description of the retrograde orthoamphibole isograd in the Limpopo Belt, South Africa, *Am. Mineral.,* 1986, vol. 71, pp. 900–915.

van Reenen, D.D. and Hollister, L.S., Fluid inclusions in hydrated granulite facies rocks, Southern Marginal Zone of the Limpopo Belt, South Africa, *Geochim. Cosmochim. Acta,* 1988, vol. 52, pp. 1057–1064.

van Reenen, D.D., Smit, C.A., Perchuk, L.L., et al., Thrust exhumation of the Neoarchean ultrahigh-temperature Southern Marginal Zone, Limpopo Complex: convergence of decompression-cooling paths in the hanging wall and prograde *P–T* paths in the footwall, *Geol. Soc. Amer. Mem.,* 2011, vol. 207, pp. 189–212.

van Reenen, D.D., Huizenga, J.-M., Smit, C.A., et al., Fluid–rock interaction during high-grade metamorphism: instructive examples from the Southern Marginal Zone of the Limpopo Complex, South Africa, *Precambrian Res.,* 2014, vol. 253, pp. 63–80.

Vennemann, T.W. and Smith, H.S., Stable isotope profile across the orthoamphibole isograd in the Southern Marginal Zone of the Limpopo Belt, South Africa, *Precambrian Res.,* 1992, vol. 55, pp. 365–397.

Vielzeuf, D., Clemens, J.D., Pin, C., et al., *Granites, granulites, and crustal differentiation, Granulites and Crustal Evolution,* Dordrecht: Kluwer Academic Publishers, 1990, pp. 59–85.

Weinberg, R.F. and Searle, M.P., The Pangong injection complex, Indian Karakorum: a case of pervasive granite flow through hot viscous crust, *J. Geol. Soc. London,* 1998, vol. 155.

Zeh, A., Jaguin, J., Poujol, M., et al., Juvenile crust formation in the northeastern Kaapvaal Craton at 2.97 Ga—implication for Archean terrane accretion, and source of the Pietersburg gold, *Precambrian Res.,* 2013, vol. 233, pp. 20–43.

Translated by E. Kurdyukov